BSPE 00295-436-5

동해 울릉분지 남부사면에서의 퇴적물 함몰구조 및 지질학적 특성 연구

(Slope Stability and Geotechnical Properties of Sediment on the Southern Margin of Ulleung Basin, East Sea(Sea of Japan))

1992. 4.

한국해양연구소

제 출 문

한국해양연구소장 귀하

본 보고서를 "동해 울릉분지 남부사면에서의 퇴적물 함몰구조 및 지질학적 특성 연구" 의 최종보고서로 제출합니다.

1992 년 4월

연구책임자 : 이 희준 (해양지질연구실)
연 구 원 : 신 동혁 (해양지질연구실)

요 약 문

I. 제목

동해 울릉분지 남부사면에서의 퇴적물 함몰구조 및 지질학적 특성 연구

II. 연구내용 및 결과

울릉분지의 남서부사면에서 길이 3 m 미만의 피스톤코아 시료를 채취하여 지질공학적분석을 시도하였고 3.5 kHz 탄성파자료와 함께 그 결과를 이 지역의 현세퇴적물의 지질공학적특성과 사면의 안정도를 진단하는데 이용하였다.

울릉분지 사면에 접한 대륙붕의 퇴적물은 대부분 집괴성의 중립내지 세립질의 모래로 구성되어 있으나, 사면퇴적물은 생물교란을 심하게 받았으며, 함수율이 높고 (170-200%), 플래스틱성질이 매우 큰 (액성한계 125-135%, plasticity index 70-80%) Silty clay로 구성되어 있다. 이들 사면퇴적물은 전형적인 반원양성니토로서 약간 과압밀되어 있으며 수축성이 매우 높다. 대부분의 지질공학적 성질들은 수심이 깊어짐에 따라 뚜렷한 변화를 보인다. 니토함량, 함수율 그리고 Atterberg limits는 깊어짐에 따라 서서히 증가하나, 탄산염함량은 상부사면에서는 약 5% 를 유지하나 깊어짐에 따라 감소하여 수심 약 1500 m 이하에서는 거의 존재하지 않는다. 총유기물함량은 전체사면에 걸쳐 비교적 일정한 값을 보인다 (8-14%). 전단응력은 수심에 따른 변화를 보이지는 않으나 대부분 지역에서 퇴적깊이에 따라 서서히 증가하는 양상을 보인다.

탄성파자료에 의하면 울릉분지 사면은 Mass wasting 에 의해 복잡한 해저지형을 보이고 있음을 알 수 있다. 상부사면에서는 사면 붕괴면과 Gully 가 빈번히 나타나고 하부사면으로 갈수록 Slide/ slump 와 Debris-flow deposit 가 우세하게 나타난다. 무한사면안정도분석에 의하면, 현재의 사면퇴적물은 정적인 배수와 비배수 조건에서 모두 안정되어 있음을 보여준다. 또한 주변의 지각운동과 관련되어 일어날 수 있는 어떠한 지진에 대해서도 동적으로 상당히 안정하다는 진단을 내릴 수 있다. 따라서 현재 사면에 놓여있는 사면붕괴물 들은 과거, 특히 해수면이 낮았을 때 (late Pleistocene) 더욱 왕성한 육상퇴적물의 사면으로의 유입과 폭풍에 의한 파도가 사면에 직접적으로 영향을 줄 수 있었던 환경에서 형성되었다고 사료된다.

SUMMARY

I. Title of Study

Slope Stability and Geotechnical Properties of Sediment on the Southern Margin of Ulleung Basin, East Sea (Sea of Japan)

II. Abstract

The Ulleung Basin is a deep back-arc basin in the East Sea. It is tectonically active in relation to the subduction zone fronting Japanese islands. High-resolution (3.5 kHz) seismic profiles and short sediment cores were obtained from the southern margin of the basin. Based on the results of geotechnical tests, pseudo-static, infinite slope stability analysis was carried out for the slope surface sediments in this region.

The shelf sediments mostly are massive, medium to fine sand, whereas on slope sediments are strongly bioturbated, water-rich (170-200% water content), and highly plastic (125-135% liquid limit; 70-80% plasticity index), silty clay. These hemipelagic muds are slightly overconsolidated and extremely highly compressible. Most geotechnical properties show distinctive downslope variations. The amount of clay fractions, water content, and Atterberg limits gradually increase downslope, whereas calcium carbonate contents decrease from 5% on the upper slope to nearly nil on the lower slope below 1500 m. Total organic matter contents are somewhat

consistent (8-14%) throughout the slope. Shear strength displays no systematic variations downslope but gradually increases downcore in most places.

Seismic data indicate that the sea floor of the slope is heavily moulded by mass wasting. A complex system of gullies and slump scars begins at the upper slope, extending to the lower slope as slide/slump and debris-flow deposits. At present, the surface sediments on the entire slope are quite stable statically under both undrained and drained conditions. They also appear to be least susceptible to slope failure by any probable earthquake loading, associated with the regionally active tectonic regime.

SLOPE STABILITY AND GEOTECHNICAL PROPERTIES OF SEDIMENT ON THE SOUTHERN MARGIN OF ULLEUNG BASIN, EAST SEA (SEA OF JAPAN)

CONTENTS

List of Figures

List of Tables

Chapter 1. INTRODUCTION

Undersea mass-wasting has played a major role in building and shaping the continental slope, particularly slopes on active margins. Although large slope instabilities are demonstrated on some of the passive margins (Embley and Jacobi, 1977; McGregor and Bennett, 1981; Jansen et al., 1987), slope failures necessarily prevail on a variety of tectonically active setting. For instances, in the Gulf of Alaska undergoing subduction, numerous mass failures have been reported to vary from slide/slump to sediment-gravity flows (Carlson and Molnia, 1978; Hampton and Bouma, 1978; Schwab and Lee, 1988). California Continental Borderland with a complex system of transcurrent faults have also abundant failed sediments on slope of basins and troughs (Edwards et al., 1980; Field and Edwards, 1980; Field et al., 1982). Likewise, mass movement deposits are widespread on the continental slope of northwest Europe near the mid-Atlantic fracture zones (Kenyon, 1987). Many causative factors govern undersea landslides, including locally high sedimentation rates, bubble-phase gas within sediments, artesian pressures in deep formations, erosional underwater currents, and cyclic stresses by waves and earthquakes (Henkel, 1970; Hampton et al., 1978; Clukey et al., 1980: Bouma, 1981; Prior and Coleman, 1984; Field and Jennings, 1987). Among them, it is the earthquake that becomes practically the most significant triggering mechanism for slope failures in the active margin.

Earthquake shocks directly stress sediments downslope. Given that the slope surface is long and continuous, an "infinite slope" assumption commonly met in submarine environments, a quasi-static force equilibrium can be simply established between external seismic forces and shear resistance of sediments, known as infinite slope stability analysis (Morgenstern, 1967; Almagor and Wiseman, 1978; Lee et al., 1981; Graham, 1984); whether or not a given slope is seismically stable could be grossly evaluated using this analysis. *In-situ* response of sediments to the seismic loading is, however, rather complicated due to occurrences of excess pore water pressure (liquefaction), and thereby to changes in the stress-strain relationship of the sediment (Poulos, 1981; Castro et al., 1985; Hamou and Kavazanjian, 1985; Poulos et al., 1985). Such a sediment behavior mobilized at the time of failure can be considerably simulated through careful laboratory measurements (static and cyclic undrained triaxial tests) (Lee, 1986).

The Ulleung Basin is a deep, bowl-shaped, back-arc basin in the East Sea (Fig. 1). The basin is tectonically active behind Japanese islands beneath which Pacific plate is being subducted. Studies of seismic profiles across the margin of the basin show that slides and slumps are ubiquitous along the slope adjacent to the continental shelf and that thick layers of mass-flow deposits (dominantly turbidites) cover the basin floor (Chough et al., 1985). The detailed distribution maps of mass-wasting features are presented on the western slope of Ulleung Basin (Chough et al., 1992) and on part of the adjacent Korea Plateau slope

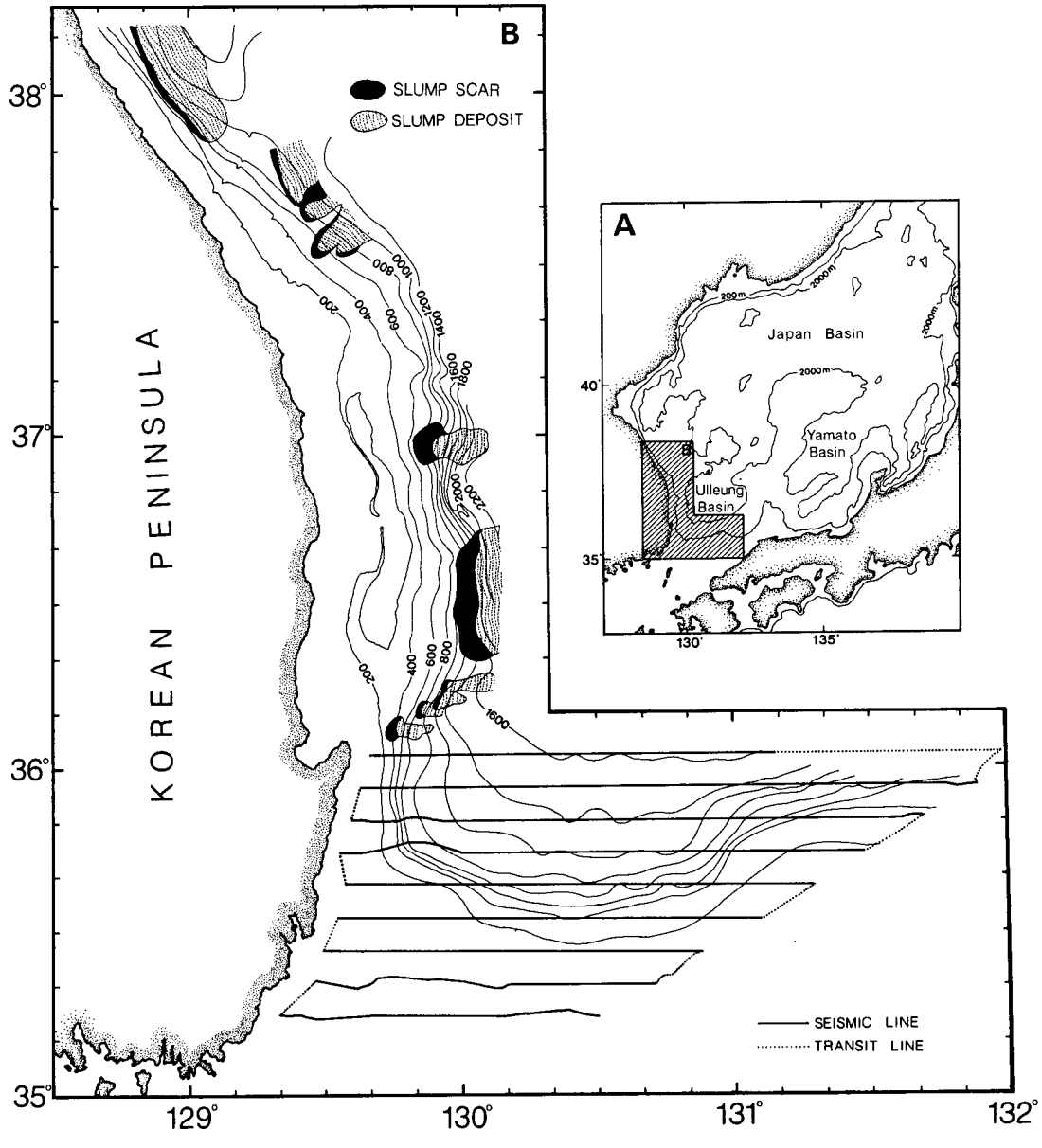

Figure 1. Map showing regional setting of Ulleung Basin (A) and the study area (B) in the East Sea (Sea of Japan). A exhibits distributions of mass wasting features on the eastern continental margin, Korea, and survey tracklines of seismic profiles in the southern margin of the Ulleung Basin. Map of mass wasting features is compiled from Lee et al. (1991) and Chough et al. (1992). Contours in meters. Details of bathymetry, tracklines, and core locations in the study area are shown in Fig. 2.

(Lee et al., 1991) (Fig. 1). These slope failures are attributed to seismic events associated with extensive faulting and folding (Chough and Lee, 1987; Lee et al., 1991). To reveal further details of geotechnical characters and stability state of the slope sediment, we conducted 3.5 kHz high-resolution seismic profiling and sediment coring on the southern margin of the basin (Figs. 1 and 2). Consolidation and static triaxial tests were performed on several core samples, in addition to standard geotechnical tests for the index properties. Based on the geophysical and geotechnical data, we attempted to achieve quantitative analyses for the slope stability in this region.

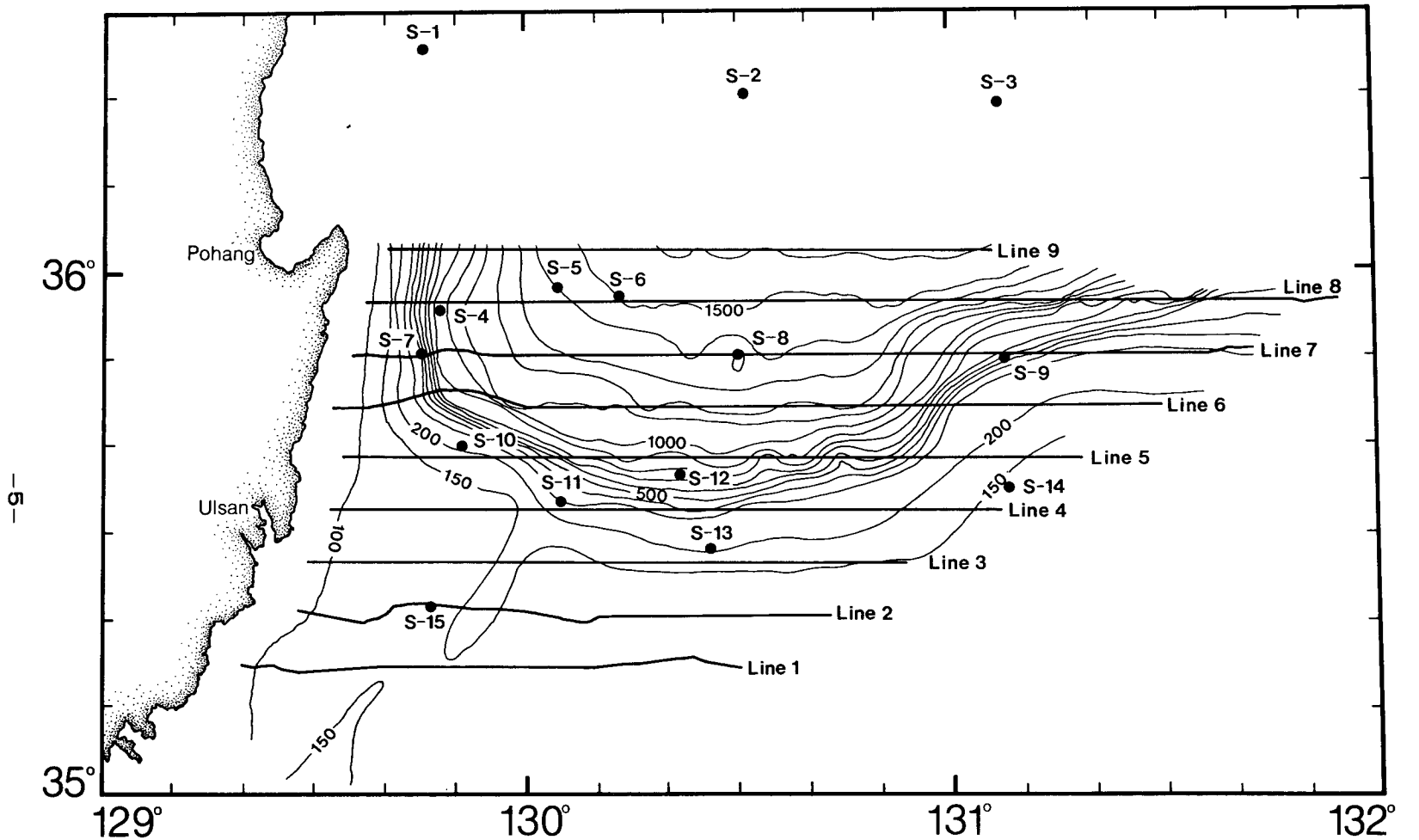

Figure 2. Bathymetric map of the study area showing survey tracklines of 3.5 kHz seismic reflection profiles and core locations (dots). Contour interval is 100 m except for the 150-m isobath. Bathymetry compiled from original soundings of this study with additions from Chough (1983).

Chapter 2. METHODS

2-1. FIELD SURVEY

High resolution (3.5 kHz) seismic profiling surveys were conducted in 1990 aboard a chartered vessel by the Korea Ocean Research and Development Institute (KORDI) using a hull-mounted ORE subbottom profiler system. The data base comprises about 1,350 line kilometers of 3.5 kHz profiles on a series of 9 east-west transects, equally spaced at 11 km (Figs. 1 and 2). Navigational control was with LORAN-C positions received every 10 min. A suite of 15 sediment cores were taken using a Benthos-type piston corer (7 cm in diameter) at selected locations for sedimentological and geotechnical analyses of the surface sediments (Fig. 2); core locations and lengths are given in Table 1.

2-2. LABORATORY TESTS

After selections of specimens for consolidation and triaxial testing, each core was split in half lengthwise and was described visually. On one half, 1-cm-thick sediment slabs were cut and X-rayed to determine detailed sedimentary structures; the other intact half was used for geotechnical analysis. Textural grain size analyses were completed by hand sieving for the >62.5 μm fraction (Carver, 1971) and by electronic particle sizing using a SEDIGRAPH model 5000D for the < 62.5 μm fraction. Grain specific gravity of oven-dried sediment was measured using an air comparison pycnometer (ASTM, 1991

Table 1. Core locations and lengths

Core number	latitude	longitude	water depth (m)	core length (cm)
S - 1	36°25.00'	129°45.00'	101	90
S - 2	36°30.58'	130°30.81'	1910	70
S - 3	36°20.09'	131°07.61'	1850	270
S - 4	35°55.44'	129°47.99'	950	210
S - 5	35°57.88'	130°05.18'	1400	200
S - 6	35°56.11'	130°12.90'	1500	170
S - 7	35°50.09'	129°45.25'	555	280
S - 8	35°50.69'	130°30.35'	1355	110
S - 9	35°49.73'	131°06.99'	650	280
S - 10	35°39.40'	129°50.85'	220	130
S - 11	35°33.99'	130°05.11'	260	150
S - 12	35°37.38'	130°21.70'	770	290
S - 13	35°31.34'	130°25.35'	230	240
S - 14	35°35.57'	131°07.96'	130	110
S - 15	35°22.03'	129°46.89'	140	70

standard D 854-83). Water content was determined gravimetrically at roughly 10 cm intervals (ASTM, 1991 standard D 2216-90); wet bulk density, void ratio, and porosity were calculated from the measured water content and grain specific gravity under the assumption of sediment water-saturation (Lee and Chough, 1987). Calcium carbonate contents were determined by a gasometric technique using a Birnard calcimeter in which approximately 1.0 g of powered and dried sediment was reacted with 5 ml of 2 *N* hydrochloric acid (Birch, 1981). Total organic matter was measured by percent weight loss by combustion at 550°C. Undrained shear strength was measured with a vane shear apparatus at a rotation rate of 60°/min. Atterberg limits (liquid and plastic limits) were determined for the selected cores following ASTM standard methods (ASTM, 1991 standard D 4318-84).

One-dimensional consolidation tests were performed in a stress-controlled mode on subsamples trimmed to 50 mm diameter and 20 mm thickness. The test data were used to calculate compression index, coefficient of consolidation, and maximum past effective overburden stress that the sediment had undergone. Also calculated were the overconsolidation ratio (OCR), the ratio of the maximum past effective overburden stress to the effective overburden stress at the time of sampling. Triaxial strength properties were obtained by static axial loading on small cylindrical samples (3.6 cm in diameter, 7.6 cm long) under undrained conditions with pore pressure measurements. The samples were consolidated to four times their estimated maximum past stress to determine the

normalized shear strength of normally consolidated sediments -- the normalized soil parameter (NSP) method (Ladd and Foott, 1974). Lee and Edwards (1986) have suggested that for predicting shear strength for deeper unsampled sediments, the NSP method is suitable where deposition has been considerably steady and uniform. This procedure not only provides a normalized shear strength that is independent of the stress state but also partly eliminates the effects of overconsolidation and mechanical disturbance upon the sediment.

Chapter 3. MORPHOLOGY

The seafloor of the basin gradually deepens northeastward to a corridor ("Ulleung Inter-plain Gap") opening to another deep basin, the Japan Basin (Fig. 1). On the western margin the slopes are regionally steep (about 4°) compared to the rest of the basin (mostly less than 2°) and bound a narrow (20 km wide) continental shelf (Fig. 1). A funnel-shaped shelf terrain encompasses the southern margin of the basin, where warm, saline waters of Tsushima Current, a branch of Kuroshio Current, enters the East Sea. Water-rich, hemipelagic sediments prevail over the slope, whereas shelf sediments are diverse in texture including gravel, sand and mud; relict sands and gravels occur near the shelf break (Fig. 3).

Based on sea floor configurations and the geotechnical characters of sediment, discussed later, the study area can be divided into 4 provinces: shelf (<300 m); upper slope (300-700 m); middle slope (700-1400 m); and lower slope (>1400 m). These topographic divisions can be regrouped into 3 seismic zones in terms of echo characters from the high-resolution (3.5 kHz) seismic data: the smooth shelf; highly rugged upper and middle slopes; and broad, hummocky lower slopes (Fig. 4).

The shelf is characterized by sharp surface echoes and few unconformably wedging or fuzzy, prolonged subbottom reflectors (Figs. 5 and 6). These echo characters probably reflect a dominance of coarse-grained materials on shelf compared to the slope sediments (Fig. 3). On the upper and middle slope

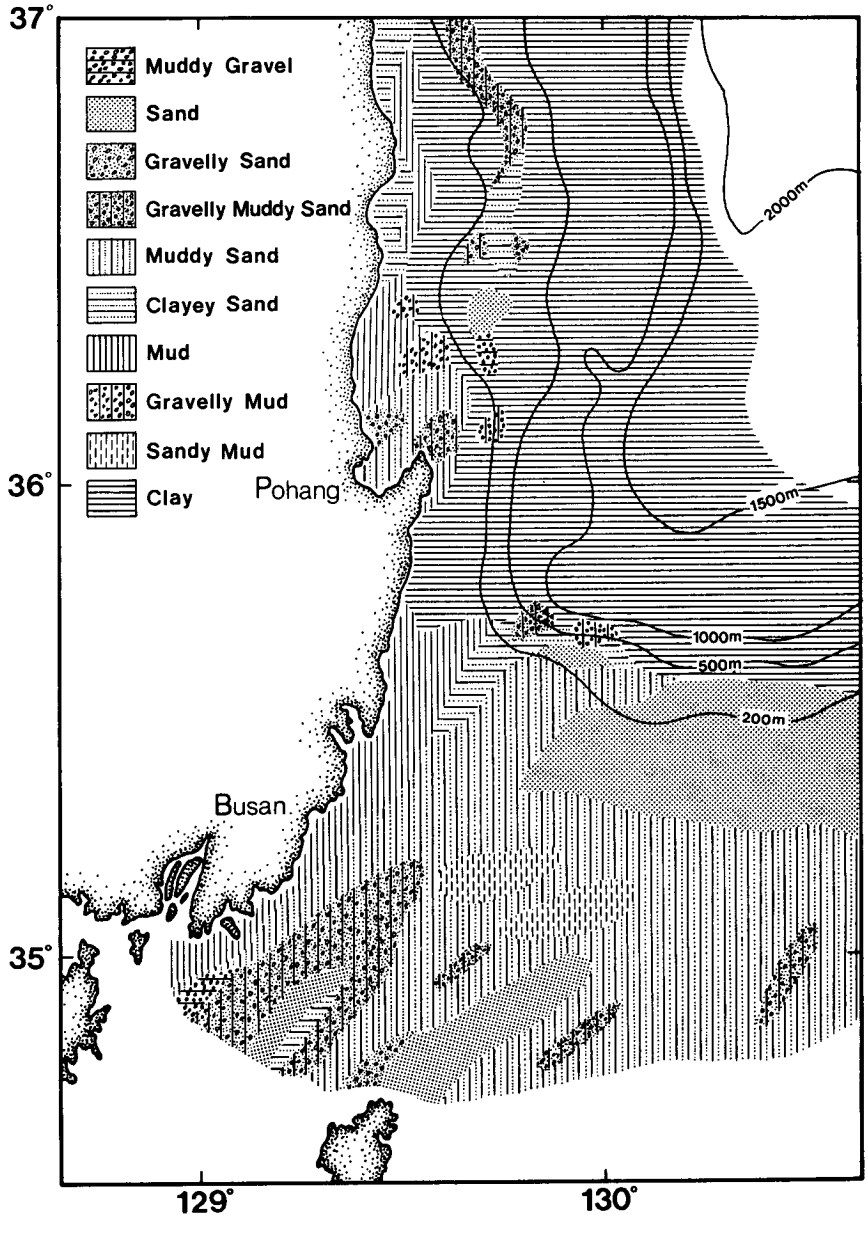

Figure 3. Map showing surface sediment distributions in the western and southern margin of the Ulleung Basin. Sediment classification from Folk's (1968) scheme. Modified from Chough (1983). Note that on shelf sediments are coarse-grained and variable in texture, whereas clayey sediments prevail over the entire slope.

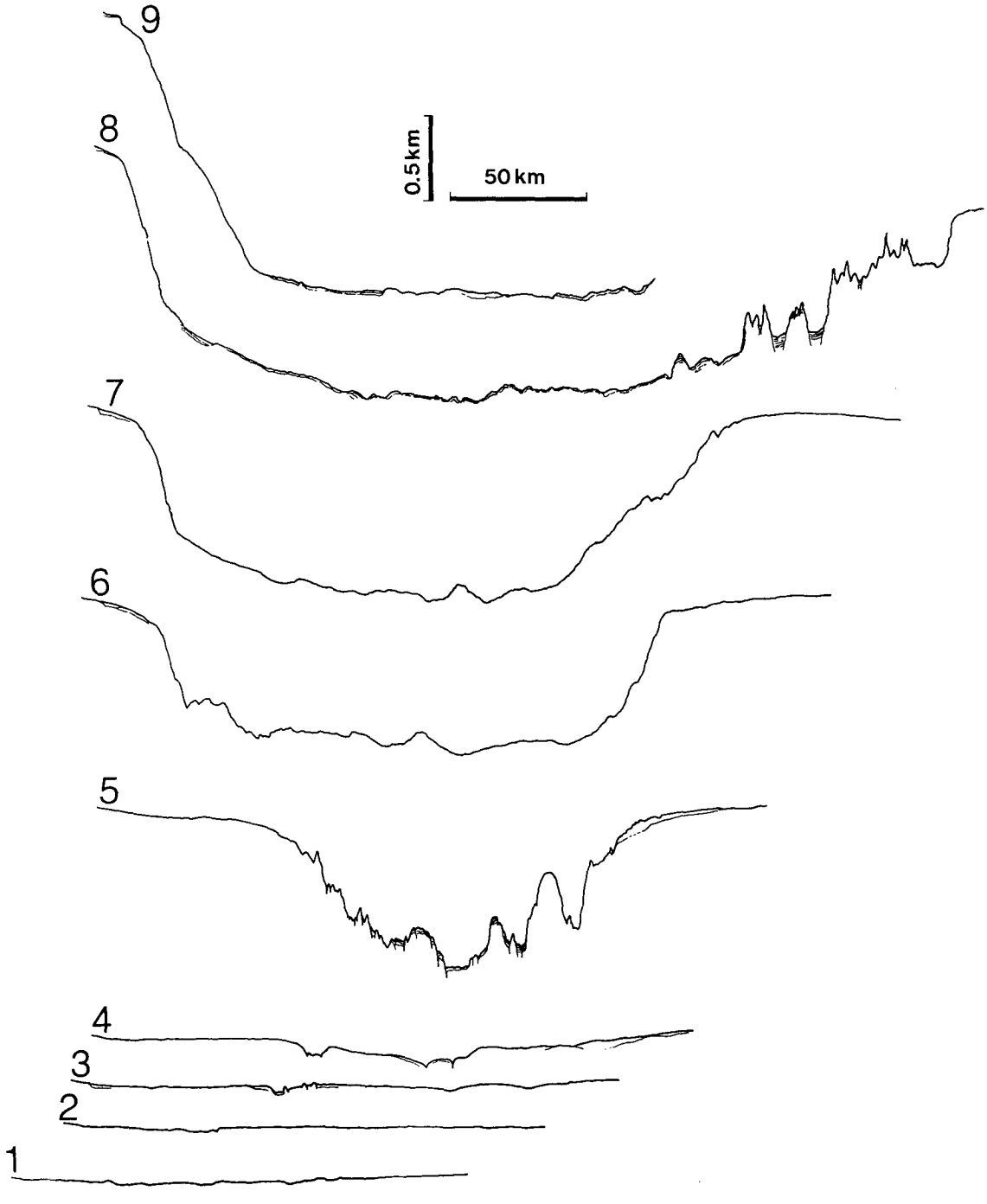

Figure 4. Line tracings of 3.5 kHz seismic reflection profiles of the southern margin of the Ulleung Basin. For accurate positions of profiles, see Fig. 2. Note that the sea floor on the eastern slope is more rugged and irregular than on the western slope. Details of shallow seismic structure are shown in Figs. 5 and 6 for profiles 5 and 8, respectively.

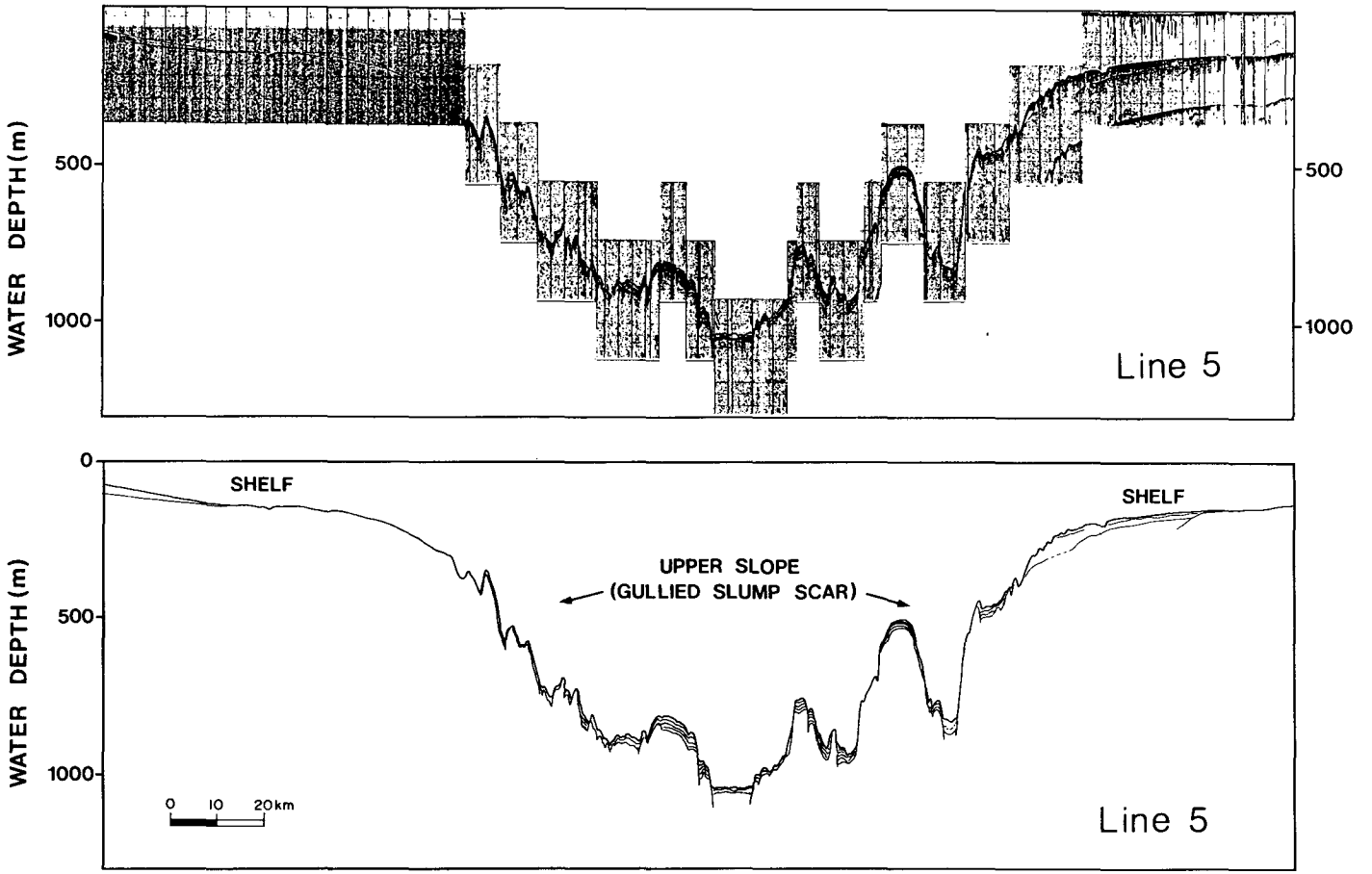

Figure 5. Original record and line drawing of the seismic profile 5 running over shelf and upper slope of the southern margin of the Ulleung Basin. Profile position on Fig. 2. The shelf is rather smooth with few unconformably wedging subbottom reflectors, whereas the upper slope is highly rugged due to abunddant mass failures (slump scar); subbottom reflectors at local steep walls are mostly truncated.

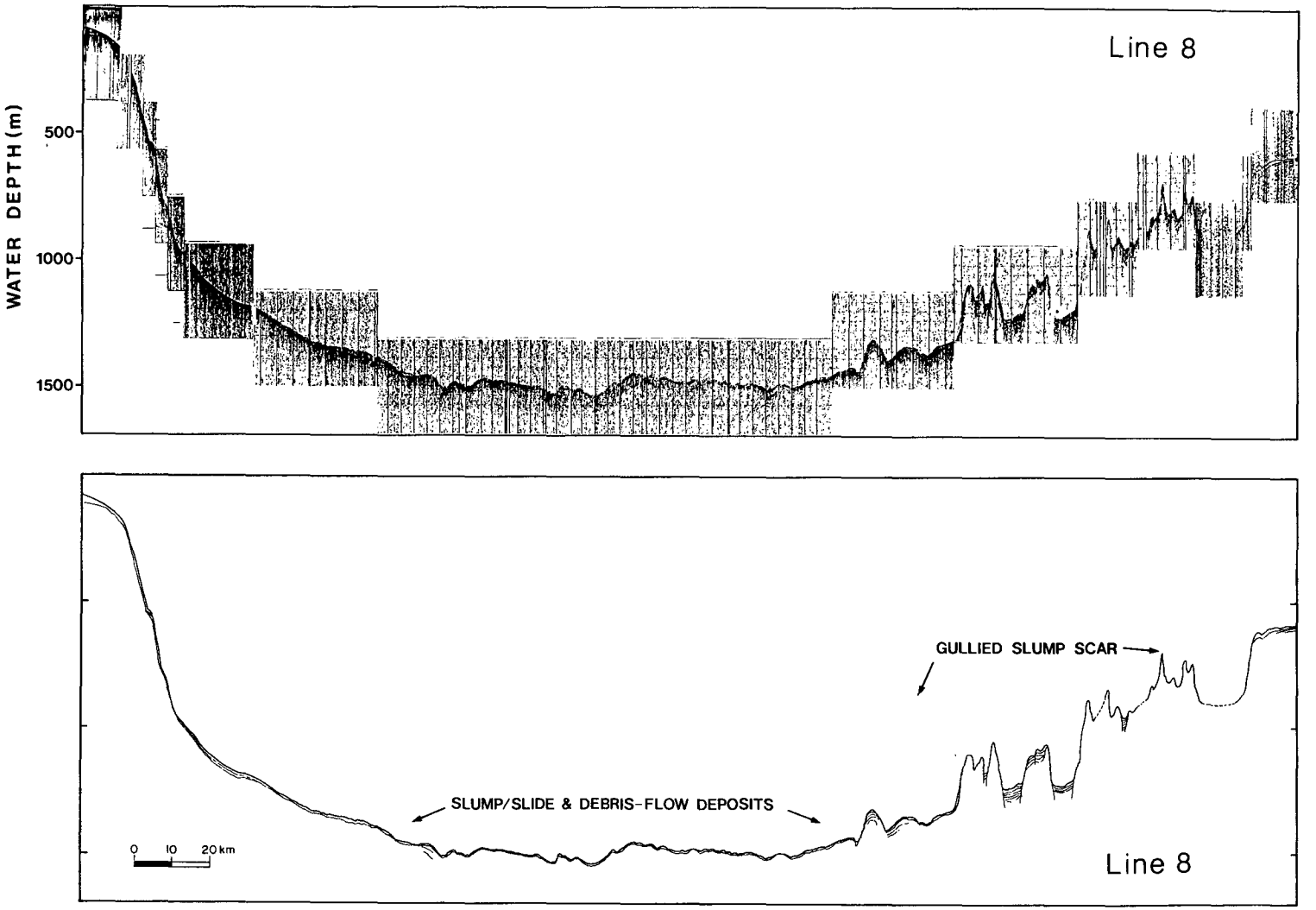

Figure 6. Original record and line drawing of the seismic profile 8 running over a whole span from shelf to lower slope on the southern margin of the Ulleung Basin. Profile position on Fig. 2. The lower slope has hummocky sea bottom and transparent subbottom layers (slide/slump and debris-flow deposits). Note that western slope is much smooth compared to complicated eastern slope.

sections, a number of topographic highs and troughs of various size comprise an irregular, high-relief morphology, although the western margin reveals greatly subdued reliefs (Figs. 4 and 6). The seismic sequences attain sharp sea-bottom echoes and parallel subbottom reflectors; the latter are mostly truncated at local steep walls and tend to be somewhat discontinuous upslope. This region appears to represent a complex morphology of gullies and slump scars eroded by vigorous activities of mass wasting. Yoon et al. (1991) also interpret similar morphologies, found on the Norwegian continental slope, as distal slope environments of the mass failure regime. The lower slope deposits have indistinct, semi-prolonged, hummocky sea-bottom echoes and subbottom transparent layers, which are often underlain by prolonged or semi-prolonged subbottom reflectors (Fig. 6). These transparent acoustic characters and hummocky surface strongly suggest slide/slump and debris flow deposits (Nardin et al., 1979; Piper et al., 1985; Lee et al., 1991; Yoon et al., 1991). In summary, the southern margin of the Ulleung Basin is heavily moulded by mass failures, which occurred on a wide range of size compared to those on the western margin of the basin and the Korea Plateau slope (cf. Lee et al., 1991).

Chapter 4. SEDIMENTARY FACIES

Based on grain-size analysis and detailed descriptions of primary sedimentary structures on X-radiographs, the sediment in the study area can be classified into 4 sedimentary facies: massive sand; bioturbated sand; bioturbated mud; and turbiditic mud.

The massive sand occurs exclusively on the shelf (Fig. 7). This facies consists of olive grey (5Y4/2), well sorted medium to fine sand, mostly containing abundant shell fragments. These shell debris are randomly oriented and tend to increase in abundance downcore. The sediment column is generally structureless with a weak to moderate degree of bioturbation (Fig. 8). Some cores on the shelfbreak (S-11 and S-14), however, are composed of highly bioturbated, well sorted, fine sands with low carbonate content, the bioturbated sand facies (Figs. 7 and 8). Chough et al. (1991) have described these types of sedimentary facies on the sea floor further south, in the deepest part of the South Sea, and interpreted them as the relict sand or the transgressive sequence formed during the early phase of the Holocene sea-level rise.

The entire cores collected from the slope predominantly show a bioturbated mud facies (Fig. 7). This facies is of strongly bioturbated, olive to dark olive (5Y3/2 or 5Y4/4), silty clay or clayey silt, suggesting uniform hemipelagic sedimentation. On the other hand, core S-3, collected from the lower slope (about 2000 m deep), involves turbiditic mud intervals of mostly volcanic ash, particularly abundant in the lower section below 200 cm subbottom (Figs. 7 and

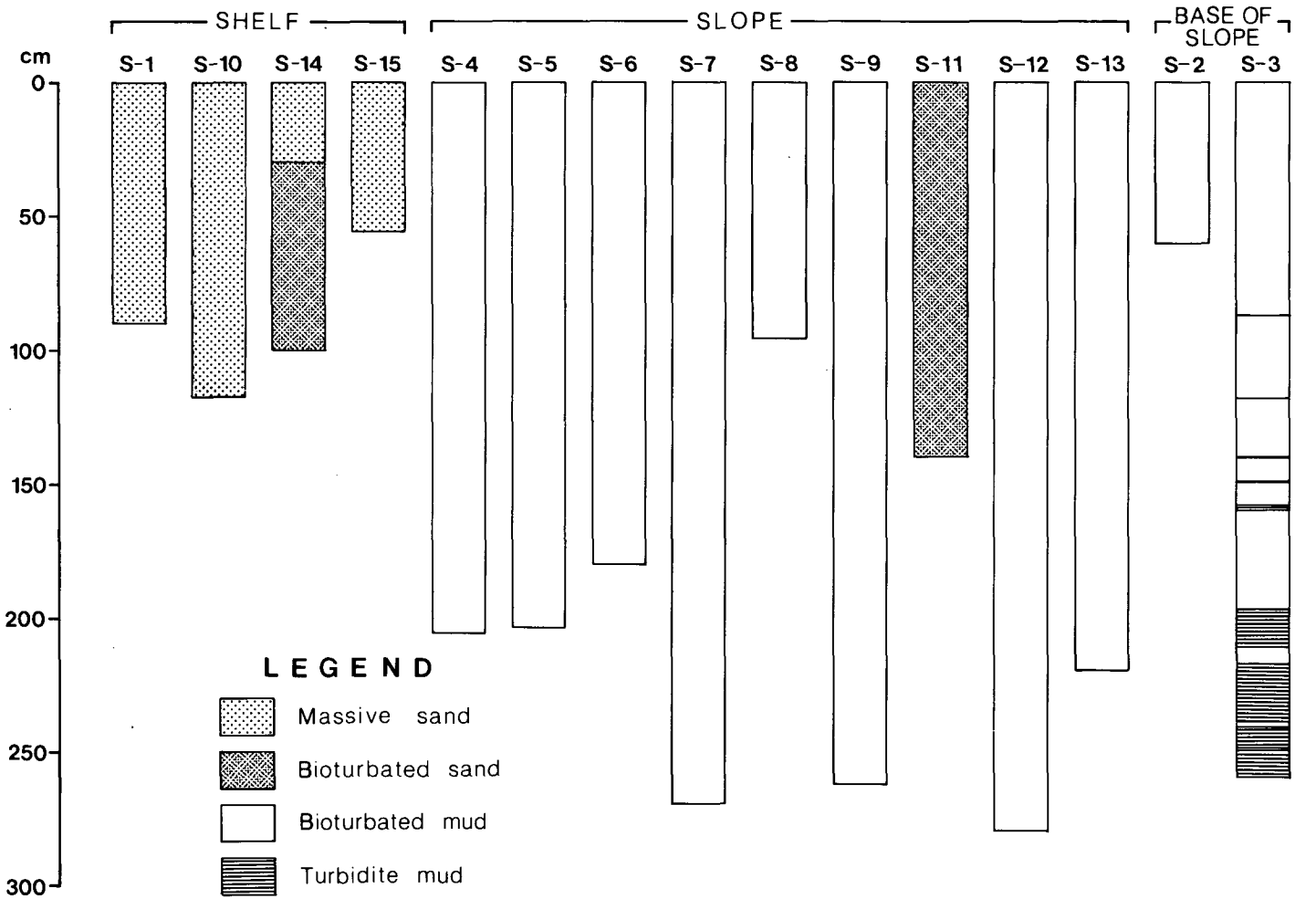

Figure 7. Core logs showing variations of sedimentary facies in different environments. Sediments on slope are dominated by strongly bioturbated, silty clayey, hemipelagic mud, in contrast to massive, medium to fine sand on the shelf. Note that near the shelf break sand and mud exist together (cores S-11 and S-13), and that a number of turbidite mud layers and laminae occur in core S-3, about 2000 m deep.

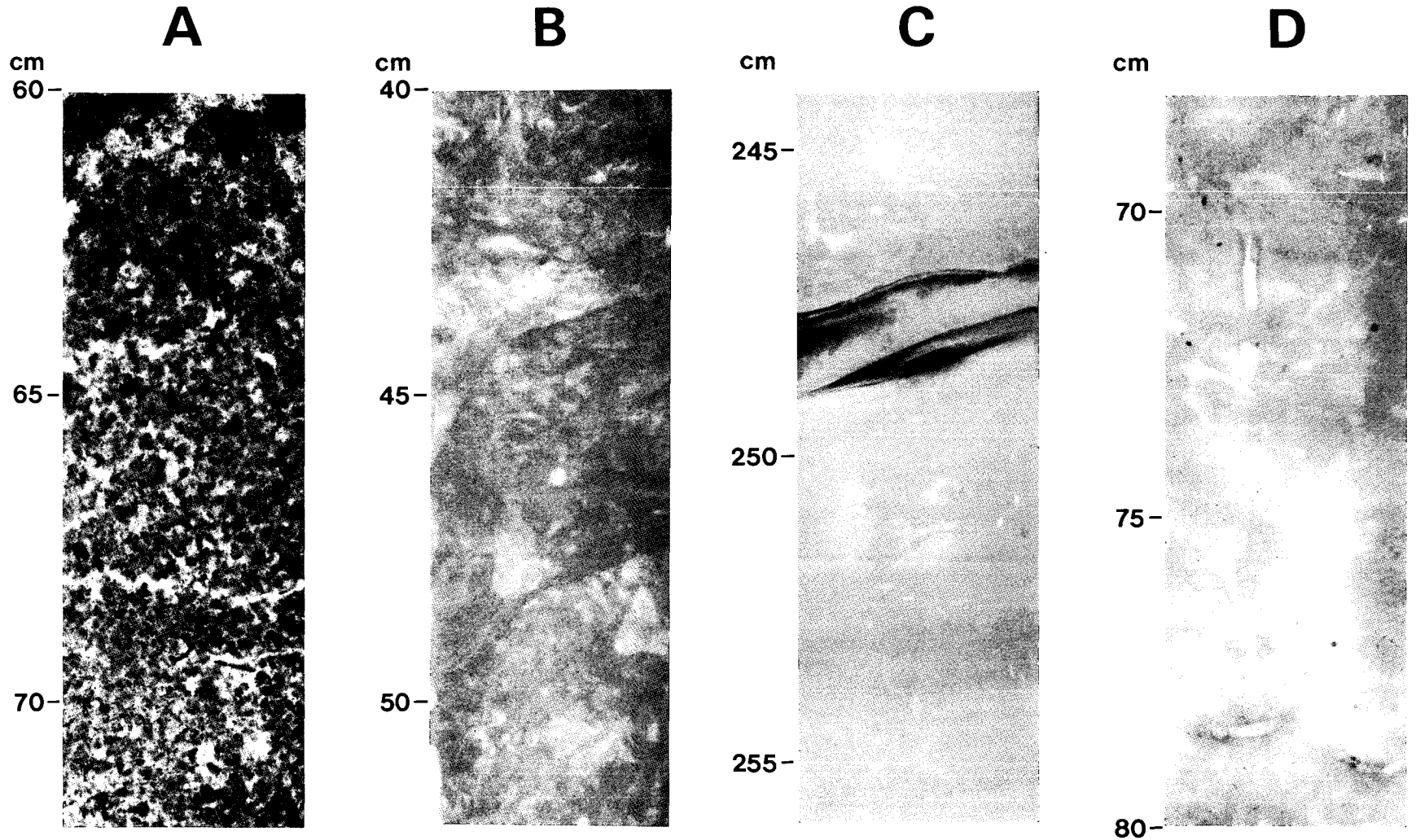

Figure 8. X-radiographs of cores representing sedimentary facies. (a) Massive sand (60-72 cm, core S-1). (b) Bioturbated sand (40-52 cm, core S-11). (c) Turbidite mud (244-256 cm, core S-3). (d) Bioturbated mud (68-80 cm, core S-12).

). The turbiditic mud facies consists of homogeneous mud or laminated mud, ;ith thicknesses varying from milimeters to several centimeters (Fig. 8); ypically, the laminated mud comprise a basal laminated silt unit and an verlying clay unit. According to the Piper's (1978) scheme, the homogeneous ıud and laminated mud can be classified as E_2 (or E_3) and E_1 divisions, espectively.

Chapter 5. GEOTECHNICAL PROPERTIES

Most geotechnical properties vary definitely with water depth. The cores retrieved are grouped into the provinces, and the average geotechnical properties for each core are given in Table 2. In addition, mean values and standard deviations for the geotechnical properties in each province are presented in Table 3.

5-1. GRAIN SIZE DISTRIBUTION

All sediments fall into the two extremely different textural types, sand and clay (or silty clay) (Fig. 9). On shelf sand predominates (mostly >95%) with abundant shell fragments, sometimes with mud chips and gravels; mean grain size ranges from 1.0 to 3.0ϕ (Table 2). The shelf sand is usually uniform in texture within 1 m below the sea floor, except for core S-1 in which mean size increases downcore from 2.5 to 0.7ϕ. Core 13, collected near the edge of the sand deposit resting on the shelf break (Figs. 2 and 3), shows topmost sands (~10 cm) and below them abruptly clayey silty columns (Table 2). Beyond shelf break sand contents sharply decrease to less than 1%, and instead clay fractions are dominant in the range of 65-85% (Table 2). Mean size shows a downslope tendency to decrease slightly from 9.0 to 9.3ϕ (Table 3). However, the turbiditic section of core S-3 has more silt fractions (~40%) and detectable sand grains (~3%) compared with clayey hemipelagic sediments in the upper section (Fig. 10).

Table 2. Average geotechnical properties of sediment cores from the southern margin of the Ulleung Basin

Province	Texture				W (%)	γ/γ	SS * (kPa)	$CaCO_3$ (%)	OM (%)	G	Atterberg limits	
	Sand	Silt	Clay (%)	Mz (ϕ)							I_p	W_l (%)
Shelf (<300m)												
core S-1	98.4	1.6	~0	1.13	27.4	0.50		12.0	2.5			
core S-10	97.2	2.8	~0	1.84	29.3	0.49						
core S-11	94.0	2.8	3.0	2.93	32.6	0.48		10.9	1.7	2.67		
core S-13												
topmost (~10 cm)	89.2	5.3	5.7	3.40	38.6	0.46		4.7	2.9			
below	19.0	46.6	34.2	7.11	75.4	0.37		11.2	7.2	2.67		
core S-14	92.9	4.4	2.4	3.03	27.5	0.50		4.0	2.2			
core S-15	97.5	2.2	~0	2.59	29.3	0.49		16.1	1.8	2.69		
Upper slope (300-700m)												
core S-7	~0	23.7	76.3	9.24	170.8	0.24	3.11	3.1	11.0			
core S-9	2.7	32.9	64.5	8.70	176.1	0.24		4.9	10.8			
core S-12	~0	31.8	67.9	9.05	154.6	0.26	3.12	4.5	9.8	2.56	69.2	127.5
Middle slope (700-1400m)												
core S-4	~0	30.3	69.6	9.06	194.6	0.22	2.58	3.3	10.2	2.61	77.9	137.8
core S-5	~0	15.5	84.6	9.62	189.6	0.23	3.61					
core S-8	~0	16.9	82.8	9.49	192.6	0.23	2.95	1.2	10.2			
Lower slope (>1400m)												
core S-2	~0	22.5	78.0	9.30	198.2	0.22	2.73	~0	10.9			
core S-3	~0	30.3	69.1	8.99	181.8	0.23	3.05	~0	11.3			
core S-6	~0	28.2	71.3	9.14	192.6	0.23	3.36	~0	11.0	2.57	82.5	134.0

W = water content; γ/γ = ratio of submerged to total bulk densities; SS = shear strength; OM = organic matter; I_p = plasticity index; W_l = liquid limit

* averaged for the upper 1 m depth

Table 3. Average (±S.D.) geotechnical properties of topmost sediments on the southern margin of Ulleung Basin

Province	Texture				W (%)	γ'/γ	SS* (kPa)	$CaCO_3$ (%)	OM (%)	G	Atterberg limits	
	Sand	Silt	Clay (%)	Mz (ϕ)							I_p	W_l (%)
Shelf	96	3	1	2.3	29.7	0.50	-	10.8	2.1	2.68	-	-
(<300m)	(3)	(1)	(2)	(0.8)	(5.1)		-	(5.6)	(0.6)	(0.02)	-	-
Upper slope	1	30	69	9.0	182.3	0.23	3.1	4.1	10.4	2.56	69.2	127.5
(300-700m)	(1)	(6)	(7)	(0.3)	(30.2)		(1.0)	(1.2)	(0.7)	(0.02)	(2.3)	(4.2)
Middle slope	~0	20	80	9.4	198.0	0.22	2.9	2.8	0.2	2.61	77.9	137.8
(700-1400m)		(7)	(7)	(0.3)	(22.0)		(1.0)	(1.3)	(0.6)	(0.04)	(1.2)	(5.1)
Lower slope	~0	24	76	9.3	195.4	0.22	3.5	~0	11.0	2.57	82.5	134.0
(>1400m)		(7)	(7)	(0.2)	(17.1)		(1.0)	-	(1.5)	(0.02)	(3.4)	(2.2)

For symbols, refer to Table 2.

* averaged for the upper 1 m depth

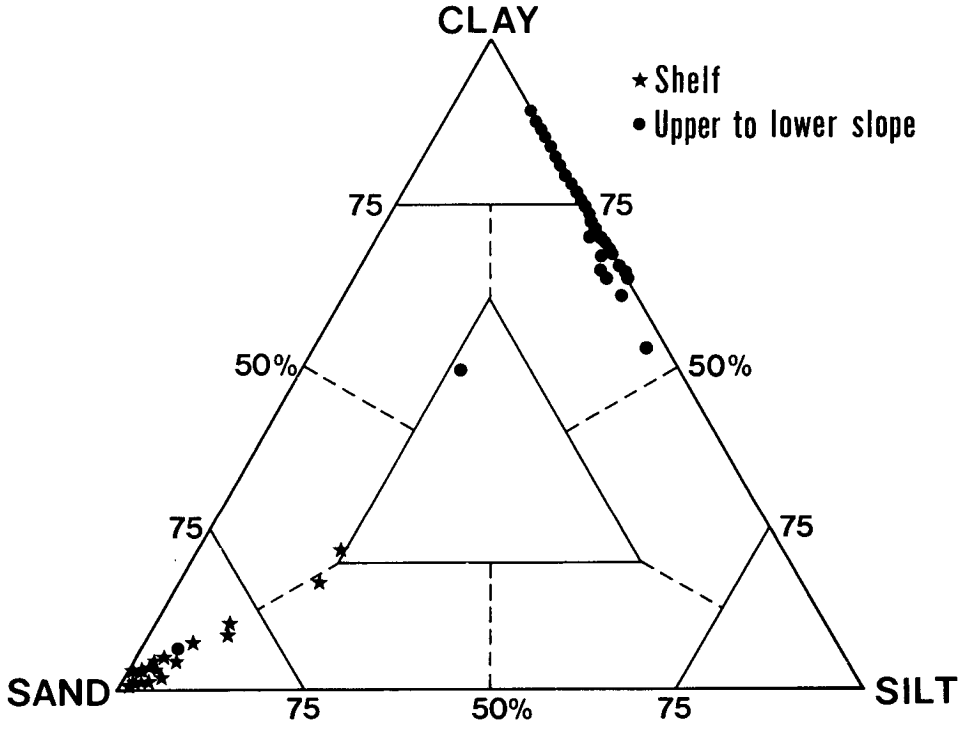

Figure 9. Grain size distribution of sediments on the southern margin of the Ulleung Basin. Notice extremely different sediment types, i.e., sand on shelf but silty clay or clay on the entire slope.

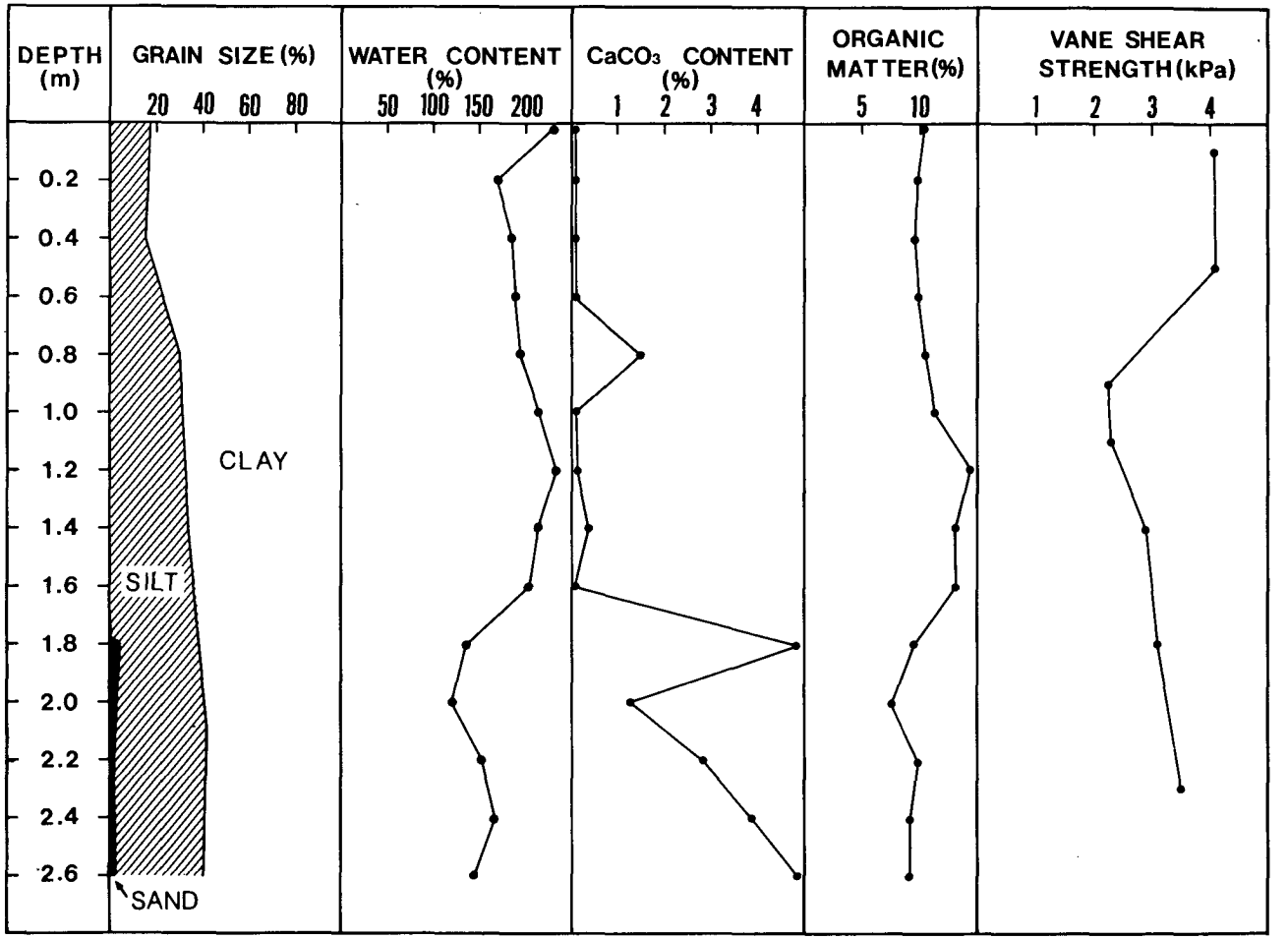

Figure 10. Profile of geotechnical properties for core S-3. Note that below 1.5 m turbidite mud shows increase in silt (and sand) and $CaCO_3$ contents but decrease in water and organic matter contents, compared to hemipelagic mud in the upper section.

5-2. WATER CONTENT

The shelf sand generally contains less than 30% of water, whereas slope muds consistently have more than 150% : there are no intermediate values between the two extremes, except for core S-13 from the shelf break (Fig. 11; Table 2). The muds tend to increase downslope in water content from 150-170% on the upper slope to more than 190% on the middle and lower slope (Table 2). With burial depth, water content of both sands and muds remains constant or slightly decreases (Fig. 11). A distinct change in water content occurs in core S-3: the upper hemipelagic muds possess about 200%, whereas the lower section with turbidites attains water content largely decreased to 150% (Fig. 10).

5-3. VANE SHEAR STRENGTH

Vane shear strength was measured only for the slope muds because vane testing is inapplicable to sands. Most of the slope cores (cores S-4, S-5, S-6, S-9, and S-12) show a downcore profile of shear strength gradually increasing from less than 1 kPa at top to more than 6 kPa below 150 cm (Fig. 11); however, core S-7 has a more or less uniform shear strength (2-4 kPa), and core S-8 even displays a downcore decreasing profile. On the lower slope the shear strength of core S-3 largely varies downcore (Fig. 10). In general, shear strength shows no convincing variations downslope (Table 2).

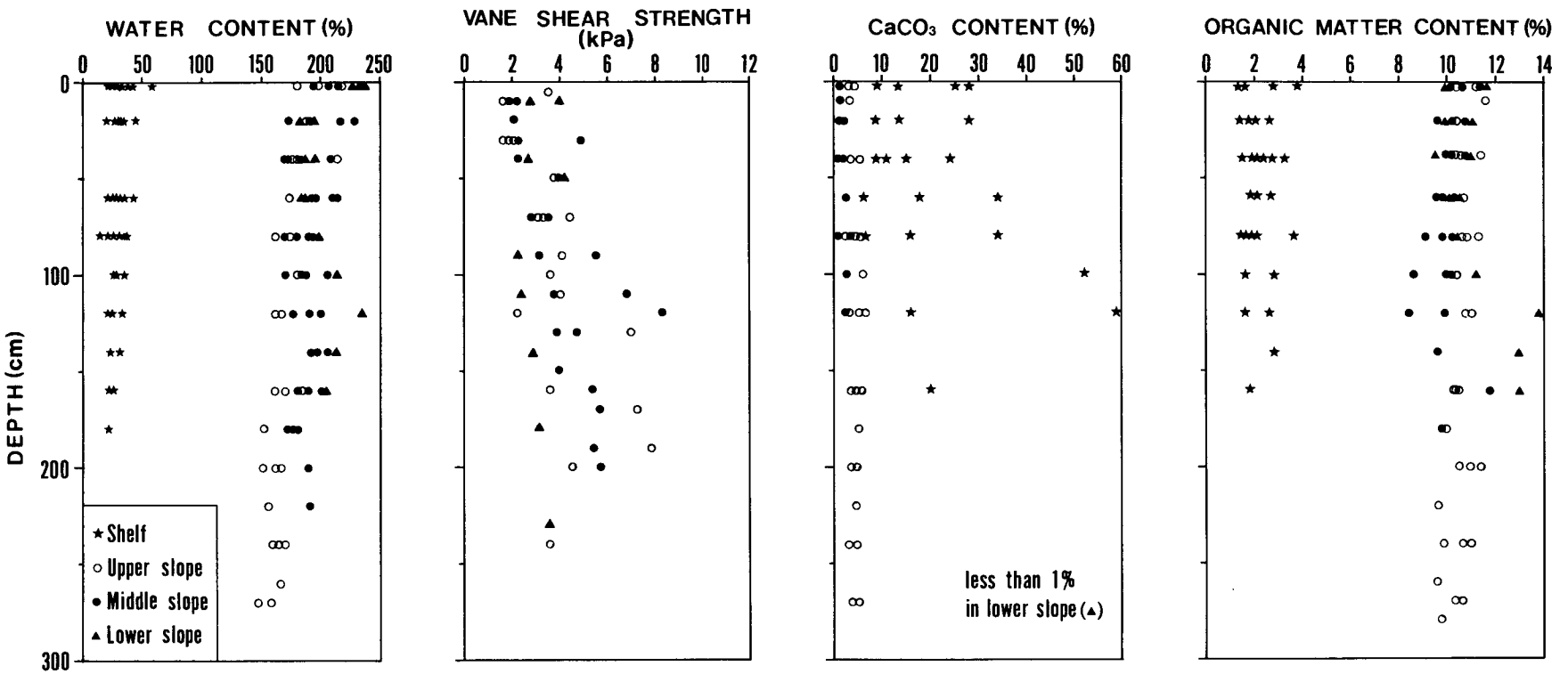

Figure 11. Geotechnical properties versus depth in core for shelf, upper slope, middle slope, and lower slope. Notice a marked diffrence in range between shelf and slope in water and organic matter contents. As a whole, water content tends to decrease gradually downcore, but vane shear strength increases steadily.

5-4. $CaCO_3$ AND ORGANIC MATTER

Most shelf sands contain a plenty of $CaCO_3$ exceeding 10% (maximum up to 60% ; Fig. 11), although core S-14 has low contents (2-5%) (Table 2). The $CaCO_3$ contents in slope muds, consistently less than 5%, slightly decrease downslope: 3-5% on the upper slope; 1-3% on the middle slope; and nearly zero on the lower slope (Tables 2 and 3). This trend is reflected in the sediment column of core S-3 in that the upper 160 cm has almost no carbonates, whereas below 160 cm the turbidites transported from upslope frequently contain more than 4% (Fig. 10). Organic contents also reveal two discrete ranges related to the sediment type: 1-4% for shelf sands; 8-14% for slope muds (Fig. 11). There is no marked trend in organic contents with both burial depth and water depth (Fig. 11; Table 3).

Grain specific gravity depends largely on the amounts of $CaCO_3$ and organic matter. The shelf sands, containing substantial amounts of $CaCO_3$ and meager organics, range in grain specific gravity from 2.65 to 2.70, whereas organic-rich, carbonate-deficient slope muds have a lowered, wide range of 2.54 to 2.65 (Tables 2 and 3).

5-5. ATTERBERG LIMITS

Atterberg limits were obtained for cores S-12, S-4 and S-6 collected on the upper, middle, and lower slopes, respectively. Liquid limit and plasticity index (liquid limit minus plastic limit) slightly increase downslope from 127 to 135%

and from 70 to 80%, respectively (Tables 2 and 3). Compared to those from the Korea Plateau slope, the liquid limit values are about 20% higher in the study area, but the plasticity index is similar between the two areas (cf. Lee et al., 1991). Within each core, Atterberg limits vary little. Plot of these data on the plasticity chart shows that the slope sediments cluster just below the A-line in the range of sediment types designated as MH (diatomaceous silty clays) or OH (organic clays of medium to high plasticity).

5-6. MECHANICAL PROPERTIES

The consolidation tests were performed on samples from cores S-12, S-4 and S-6 (all 1.2 m depth in core). The results indicate that all samples are slightly overconsolidated with the OCR of 2 to 4. The compression index (C_c), the change in void ratio that occurs during a tenfold increase in vertical effective stress, varies between 1.11 and 1.86; high values are from the middle slope. This range indicate that the Ulleung Basin slope sediment is extremely highly compressible, beyond the limits documented for marine sediments elsewhere: $0.20<C_c<0.87$ (Richards, 1962); $0.06<C_c<1.11$ (Hampton, 1989). The coefficient of consolidation (c_v) is generally less than 0.1×10^{-2} cm^2/sec.

Static undrained triaxial tests were conducted on samples taken at the interval of 1.0 to 1.5 m in cores S-12, S-4 and S-6. The samples were preconsolidated isometrically according to the NSP method. The ratio, S, of the undrained shear strength to the consolidation stress increases downslope from 0.62

through 0.89 to 1.30 for cores S-12, S-4, and S-6, respectively. The effective angle of internal friction (ϕ') is identical at 18° for cores S-12 and S-4 but increases to 23° for core S-6.

Chapter 6. SLOPE STABILITY ANALYSIS

Slope-failure susceptibility for the uppermost sediment in the study area is evaluated tentatively, based on the triaxial measurements of cores S-12, S-4, and S-6. The triaxial strength properties measured appear to be relatively reproducible. The least square fits of the vertical profile of vane shear strength, measured on the rest of the three cores, yield limiting values of S, 0.64, 0.69, and 1.28 respectively (Fig. 12), well confirming the triaxial measurements. Furthermore, another middle slope core (S-5) also provides a value of 0.64 for S. In this respect, the three cores S-14, S-15, and S-16 should have little disturbance by coring, and the measured mechanical properties seem to be fairly reliable.

The slope stability under undrained gravitational loading conditions only can be grossly evaluated by calculating a simple factor of safety (F):

$$F = S/(\sin\alpha \cos\alpha)$$

where α is the slope angle of the seafloor. $F > 1.0$ indicates stability, whereas $F < 1.0$ indicates instability.

On the upper slope the slope gradient is approximately 1°, and a value of S from core S-12 amounts to 0.62, which gives $F >> 1.0$. This implies that the upper slope sediments are quite stable under static undrained (rapid) loading conditions. Under static drained (long-term) loading conditions, this area also is much stable because the maximum stable slope for a fully drained gravitational loading is equal to ϕ' (Edwards et al., 1980); the frictional angle is

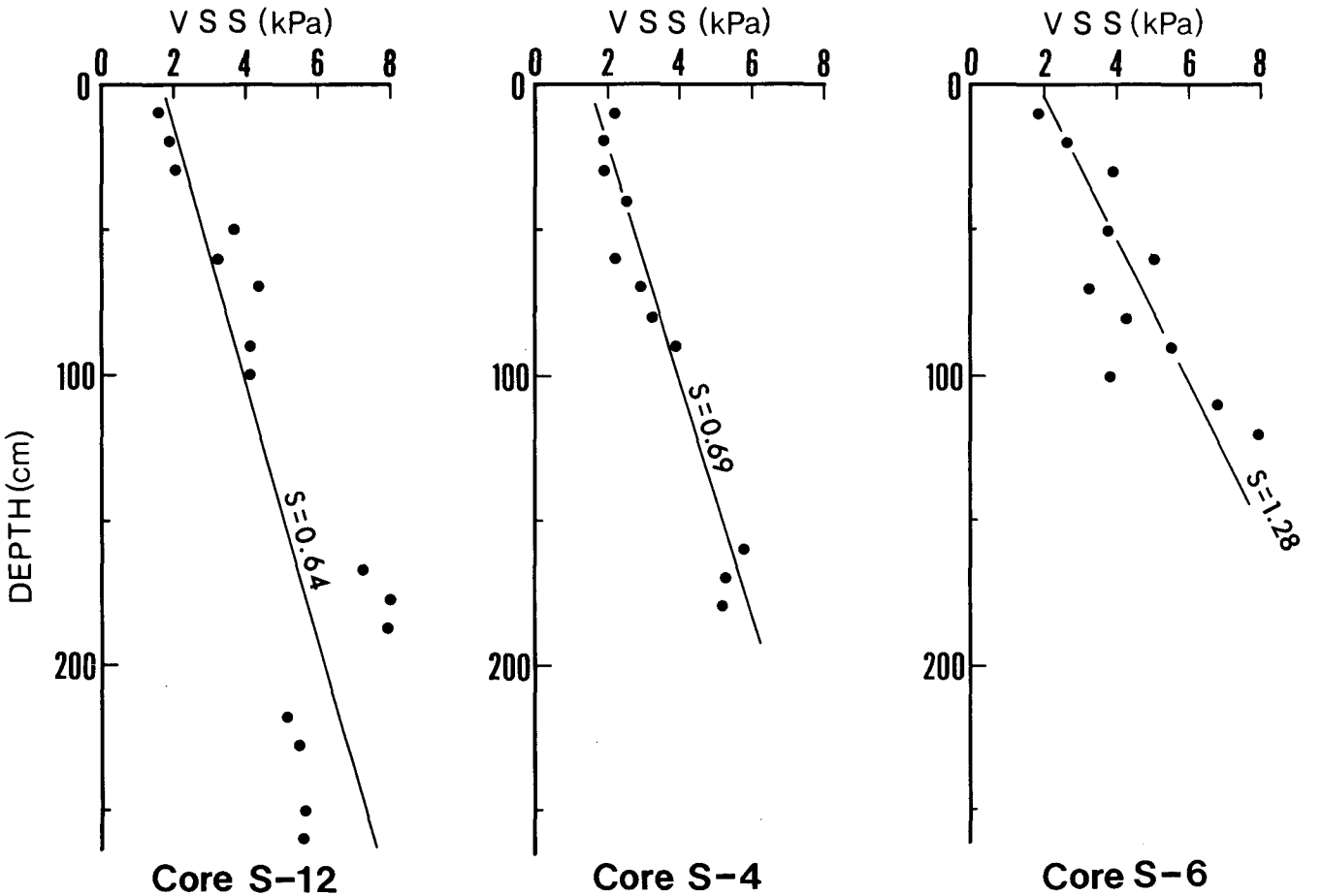

Figure 12. Vane shear strength (VSS) versus depth in core for cores S-12, S-6, and S-4. The limiting values of S from least square fitting well confirms triaxial measurements (see text).

18° on the upper slope. Similarly, calculating the safety equation for the middle and lower slope with the corresponding data sets (S = 0.89, 1.30; the slope angle = 4, 1°; ϕ'= 18, 23°, respectively) also indicates that the middle and lower slope sediments are quite stable statically under both drained and undrained loading conditions. These results additionally show that the entire slope is more stable under undrained static conditions compared to drained conditions. Some possible exceptions, however, will exist on some localized walls of canyons or gulleies: sediments on an oversteep slope far exceeding 18° might have been failed or have a great potential for static drained failure.

The effects of earthquake loading can be evaluated by the method of Lee and Edwards (1986) modified from Morgenstern (1967) and Seed and Rahman (1978):

$$k_c = (\gamma'/\gamma)[A_c A_d US\ (OCR)^m - \sin\alpha]$$

where k_c is the critical pseudo-static horizontal earthquake acceleration (expressed as a percent of gravity) required to cause failure, A_c is a correction factor for the difference between shear strengths under isotropic (laboratory) and anisotropic (field) confining pressure, A_d is a correction factor for static-strength degradation by cyclic loads, U is the degree of consolidation (U=1 for normal and overconsolidation and is <1 for underconsolidation), m is a sediment parameter (typically equal to about 0.8), and γ'/γ is the ratio of submerged to total bulk densities.

Since the parameters A_c and A_d were not directly evaluated from cyclic loading tests, we determined the most probable range of them based on the results documented elsewhere. Lee (1986) reports that A_c typically ranges between 0.8 and 1.0 for marine fine-grained sediments, being supported by Hampton (1989). Hampton's (1989) cyclic strength-test results for the terrigenous and diatom-rich sediments on the Kodiak shelf, Alaska show that A_d is generally larger than 0.8. On the Ebro margin, western Mediterranean, Baraza et al. (1990) obtained a value of 1.19 for A_c and a range of 0.73 - 1.53 for A_d. Therefore, although with limited validity, the range of 0.8-1.0 for both A_c and A_d seems most appropriate for this analysis. From Table 3, $\gamma'/\gamma = 0.22$. The effects of overconsolidation, whether it is true or apparent, diminishes so rapidly with subbottom depth that the sediment several tens of meters deep must be nearly normally consolidated, i.e., OCR=1. As a result, the calculated values of k_c are in the ranege of 0.08-0.13, 0.12-0.18, and 0.18-0.28 for the upper, middle, and lower slopes, respectively. This suggests that the surficial sediments of the upper slope have the greatest relative susceptibility to slope failure by repeated loading from earthquakes.

Chough and Lee (1987) have assessed the stability of the upper slope sediments near Pohang with vane shear strength data, giving a critical horizontal acceleration of 0.09; this value is favorably comparable with that for the upper slope in the present study area. Using Facciolis' (1977) equation, they have derived a critical earthquake intensity of 5 and concluded that the upper slope

sediment therein is metastable under continued activities of the adjacent Yansan Fault on land, the nearest probable seismic center around the western and southwestern margin of the Ulleung Basin. For the present study area, however, the Facciolis' equation yields an increased critical value greater than 7.0, because its distance from the Yansan Fault is 500 km or more compared to about 100 km for the area of Chough and Lee (1987). The 1905-1982 seismic measurements near the Yansan Fault indicate no strong earthquakes greater than 5.0, although tens of minor seismic events have occurred (Lee et al., 1984). Consequently, the preliminary results of the analysis suggest that the slope sediments in the southern margin of the Ulleung Basin appear to be presently stable -- seismically as well as statically. In this respect, the mass wasting features found ubiquitously on the basin slope would be largely remnants of ancient slope failures, most probably having occurred during the Pleistocene lower-stand of sea levels when the terrigeneous materials may have been more actively transported to the slope, and storm waves may have substantially affected the upper slope sediments, with continual triggering by tectonic movements.

Chapter 7. CONCLUSIONS

The surface sediments on the southern slope of the Ulleung Basin are dominated by strongly bioturbated, silty clayey, hemipelagic muds, in contrast to massive, medium to fine sand on the shelf. The slope muds reveal distinctive downslope variations in most geotechnical properties. Clay fractions slightly increase from 70% on the upper slope to 80% on the lower slope, and water contents accordingly increase downslope from 170 to 200%. These watery, clayey sediments attain very high plasticity, ranging between 125 and 135% in liquid limit and between 70 and 80% in plasticity index; within these ranges, both quantities tend to increase downslope. On the other hand, calcium carbonate contents, about 5% on the upper slope, steadily decrease downslope to nearly nil on the lower slope below 1500 m, and total organic matter contents are consistent (8-14%) throughout the slope. The slope muds are slightly overconsolidated and extremely highly compressible. Shear strength gradually increases downcore in most places but shows no systematic variations downslope.

High-resolution (3.5 kHz) seismic data indicate that the sea floor configurations comprise the smooth shelf, highly rugged upper and middle slope, and broad, hummocky lower slope. Such a complicated morphology appears to have formed by vigorous activities of mass wasting, resulting in gullies and slump scars on the upper and middle slope and slide/slump and debris-flow deposits on the lower slope. The results of infinite slope stability,

however, suggest that at present the surface sediments on slope are quite stable statically under both undrained and drained conditions. This analysis also suggests their least susceptibility to slope failure by any probable earthquakes associated with the regionally active tectonic regime in the western and southern margin of the Ulleung Basin.

ACKNOWLEDGMENTS

This study was supported through grants to Lee (Basic Research Project PE00295) by the Korea Ocean Research and Development Institute. D.H. Shin, S. Chang, and G.S. Kim assisted with field work and laboratory analyses. Consolidation tests and triaxial compression tests were conducted at the geotechnical laboratory of the Department of Soil Engineering at the Seoul National University. All this help is gratefully acknowledged.

REFERENCES

Almagor, G and Wiseman, G., 1978. Analysis of submarine slumping in the continental slope off the southern coast of Israel. Mar. Geotechnol., 2: 349-388.

American Society for Testing and Materials (ASTM), 1991. Annual Book of ASTM Standards, Vol. 04.08, Soil and Rock, Dimension Stone, and Geosynthetics. Philadelphia, ASTM, 1182pp.

Baraza, J., Lee, H.J., Kayen, R.E. and Hampton, M.A., 1990. Geotechnical characteristics and slope stability on the Ebro margin, western Mediterranean. Mar. Geol., 95: 379-393.

Birch, G.F., 1981. The Karbonat-bombe: a precise, rapid and cheap instrument for determining calcium carbonate in sediments and rocks. Trans. Geol. Soc. S. Afr., 84: 199-203.

Bouma, A.H., 1981. Introduction to offshore geologic hazards. In: A. Bouma, D. Sangrey, J. Coleman, D. Prior, A. Trippet, W., Dunlap and J. Hooper (Editors), Offshore Geologic Hazards. Offshore Technol. Conf. Educ. Course Note Ser., 18: 1-101.

Carlson, P.R. and Molnia, B.F., 1978. Submarine faults and slides on the continental shelf, northern Gulf of Alaska. Mar. Geotechnol., 2: 275-290.

Carver, R.E., 1971. Procedure in Sedimentary Petrology. Wiley-Interscience, New York, 653pp.

Castro, G., Polous, S.J. and Leathers, F.D., 1985. Re-examination of slide of Lower San Fernando Dam. J. Geotechnical Eng. ASCE, 111: 1093-1107.

Chough, S.K., 1983. Marine geology of Korean Seas. Int. Hum. Resour. Dev. Corp., Boston, Mass., 157pp.

Chough, S.K. and Lee, H.J., 1987. Stability of sediments on the Ulleung basin slope. Mar. Geotechnol., 7: 123-132.

Chough, S.K., Jeong, K.S. and Honza, E., 1985. Zoned facies of mass-flow deposits in the Ulleung (Tsushima) basin, East Sea (Sea of Japan). Mar. Geol., 65: 113-125.

Chough, S.K., Lee, H.J. and Han, S.J., 1991. Sedimentological and geotechnical properties of fine-grained sediments in part of the South Sea, Korea. Cont. Shelf Res., 11: 183-195.

Chough, S.K., Lee, H.J. and Yoon, S.H., 1992. Submarine slides in the eastern continental margin, Korea. Mar. Geotechnol. (in press).

Clukey, E., Cacchione, D.A. and Nelson, H., 1980. Liquefaction potential of the Yukon prodelta, Bering Sea. Offshore Technol. Conf., 12th, pp. 315-325.

Edwards, B.D., Field, M.E. and Clukey, E.C., 1980. Geological analysis of a submarine slump, California borderland. Offshore Technol. Conf., 12th, pp. 399-410.

Embley, R.W. and Jacobi, R.D., 1977. Distribution and morphology of large submarine sediment slides and slumps on Atlantic continental margins. Mar. Geotechnol., 2: 205-227.

Facciolis, E., 1977. Site dependent probability distributions for peak ground motion parameters in strong earthquakes. Rep. E23, Instituto de Ingenieria, U.N.A.M. (Mexico).

Field, M.E. and Edwards, B.D., 1980. Slopes of the southern California borderland: a regime of mass transport. In: M.E. Field, I.P. Colburn and A.H. Bouma (Editors), Quaternary Depositional Environments of the Pacific Coast, SEPM, Los Angeles, pp. 169-184.

Field, M.E. and Jennings, A.E., 1987. Seafloor gas seeps triggered by a northern California Earthquake. Mar. Geol., 77: 39-51.

Field, M.E., Gardner, J.V., Jennings, A.E. and Edwards, B.D., 1982. Earthquake-induced sediment failures on a 0.25° slope, Klamath River delta, California. Geology, 10: 542-546.

Fork, R.L., 1968. Petrology of Sedimentary Rocks. Austin, Texas, Hemphill's, 170p.

Graham, J., 1984. Methods of stability analysis. In: D. Brunsden and D.B. Prior (Editors), Slope Instability. Wiley, New York, pp. 171-215.

Hamou, T.H. and Kavazanjian, E., Jr., 1985. Seismic stability of gentle infinite slopes. J. Geotechnical Eng., 111: 681-697.

Hampton, M.A., 1989. Geotechnical properties of sediment on the Kodiak continental shelf and upper slope, Gulf of Alaska. Mar. Geotechnol., 8: 159-180.

Hampton, M.A. and Bouma, A.H., 1978. Slope instability near the shelf break, western Gulf of Alaska. Mar. Geotechnol., 2: 309-331.

Hampton, M.A., Bouma, A.H., Carlson, P.R., Molnia, B.F., Clukey, E.C.and Sangrey, D.A., 1978. Quantitative study of slope instability in the Gulf of Alaska. Offshore Technol. Conf., 10th, pp. 2307-2318.

Henkel, D.J., 1970. The role of waves in causing submarine landslides. Geotechnique, 20: 75-80.

Jansen, E., Befring, S., Bugge, T., Eidvin, T., Holtedahl, H. and Sejrup, H.P., 1987. Large submarine slides on the Norwegian continental margin: sediments, transport and timing. Mar. Geol., 78: 77-107.

Kenyon, N.H., 1987. Mass-wasting Features on the continental slope of northwest Europe. Mar. Geol., 74: 57-77.

Ladd, C.C. and Foott, R., 1974. New design procedure for stability of soft clays. J. Geotechnical Eng. Div., ASCE, 100: 763-786.

Lee, H.J., 1986. State of the art: laboratory determination of the strength of marine soils. Spec. Technical Publ. 883, ASTM, Vol. 1, pp. 181-250.

Lee, H.J. and Chough, S.K., 1987. Technical note -- bulk density, void ratio, and porosity determined from average grain density and water content: an evaluation errors. Mar. Geotechnol., 7: 53-62.

Lee, H.J. and Edwards, B.D., 1986. Regional method to assess offshore slope stability. J. Geotechnical Eng., 112: 489-509.

Lee, H.J., Edwards, B.D. and Field, M.E., 1981. Geotechnical analysis of a submarine slump, Eureka, California. Offshore Technol. Conf., 13th, pp. 53-65.

Lee, H.J., Chough, S.K., Chun, S.S. and Han, S.J., 1991. Sediment failure on the Korea Plateau slope, East Sea (Sea of Japan). Mar. Geol., 97: 363-377.

Lee, K., Jeong, B., Kim, Y. and Yang, S.J., 1984. A geophysical study of the Yangsan Fault area. J. Geol. Soc. Korea, 20: 222-240.

McGregor, B.A. and Bennett, R.H., 1981. Sediment failure and sedimentary framework of the Wilmington geotechnical corridor, U.S. Atlantic continental margin. Sediment. Geol., 30: 213-234.

Morgenstern, N.R., 1967. Submarine slumping and the initiation of turbidity currents. In: A.F. Richards (Editor), Marine Geotechnigue, Univ. Illinois Press, Urbana, pp. 189-210.

Nardin, T.D., Hein, F.J., Gorsline, D.S. and Edwards, B.D., 1979. A review of mass movements processes, sediment and acoustic characteristics, and contrasts in slope and base-of-slope systems versus canyon-fan-basin floor systems. In: L.J. Doyle and O.H. Pilkey (Editors), Geology of Continental Slopes. Soc. Econ. Paleontol. Mineral. Spec. Publ., 27: 61-73.

Piper, D.J.W., 1978. Turbidite muds and silts in deep-sea fans and abyssal plains. In: D.J. Stanley and G. Kelling (Editors), Sedimentation in Submarine Fans, Canyons, and Trenches. Dowden, Huchinson and Ross, Stroudsburg, Penn., pp. 163-176.

Piper, D.J.W., Farre, J.A. and Shor, A., 1985. Late Quaternary slumps and debris flows on the Scotian Slope. Geol. Soc. Am. Bull., 96: 1508-1517.

Poulos, S.J., 1981. The steady state of deformation. J. Geotechnical Eng. ASCE, 107: 553-562.

Poulos, S.J., Castro, G. and France, J.W., 1985. Liquefaction evaluation procedure. J. Geotechnical Eng. ASCE, 111: 772-791.

Prior, D.B. and Coleman, J.M., 1984. Submarine slope instability. In: D. Brunsden and D.B. Prior (Editors), Slope Instability. Wiley, New York, pp. 419-455.

Richards, A.F., 1962. Investigation of deep-sea sediment cores, II. Mass physical properties. U.S. Navy Hydrog. Office Technical Rep. 106, 146pp.

Schwab, W.C. and Lee, H.J., 1988. Causes of two slope-failure types in continental-slope sediment, northeastern Gulf of Alaska. J. Sediment. Petrol., 58: 1-11.

Seed, H.B. and Rahman, M.S., 1978. Wave-induced pore pressure in relation to ocean floor stability of cohesionless soils. Mar. Geotechnol., 3: 123-150.

Yoon, S.H., Chough, S.K., Thiede, J. and Werner, F., 1991. Late Pleistocene sedimentation on the Norwegian continental slope between 67° and 71° N. Mar. Geol., 99: 187-207.

APPENDIX. Summary Geotechnical Properties of Cores from the Southern Margin of the Ulleung Basin

Core	Depth		Texture (%)		Mean	Stand.	Water c.	Bulk d.	Void	Porosity	Shear str.	Specific	CaCO3	Org.	Att	erberg	L. (%)	Ac
No.	(cm)	Sand	Silt	Clay		Dev.	(%)	(g/cm3)	ratio	(%)	(kPa)	gravity	(%)	matt.(%)	PL	LL	PI	
S-1	0	94.4	5.6	0.0	2.49	0.82	41.9	1.80	1.11	52.61			25.3	3.8				
101m	10																	
	20	99.2	0.8	0.0	1.17	0.76	32.0	1.91	0.85	45.89			13.2	2.6				
	30																	
	40	99.4	0.6	0.0	0.87	0.68	27.8	1.97	0.74	42.42			8.6	2.3				
	50																	
	60	99.6	0.4	0.0	0.40	0.80	21.3	2.07	0.56	36.08			6.2	2.1				
	70																	
	80	99.4	0.6	0.0	0.70	1.01	13.9	2.22	0.37	26.92			6.5	1.9				
	Ave.	98.4	1.6	0.0	1.13	0.81	27.4	2.00	0.73	40.78			12.0	2.5				
	S.D.	2.0	2.0	0.0	0.81	0.11	10.6	0.16	0.28	9.79			8.0	0.8				
S-2	0	0.2	20.8	79.0	9.27	1.56	226.4	1.26	6.00	85.71				11.5				
1910m	10										2.77		~0					
	20						187.2	1.30	4.96	83.22			~0	10.8				
	30																	
	40						195.3	1.29	5.18	83.81	2.69		~0	10.8				
	50	0.4	22.7	76.9	9.20	1.62												
	60						183.9	1.31	4.87	82.97			~0	10.5				
	Ave.	0.3	22.5	78.0	9.30	1.59	198.2	1.29	5.25	83.93	2.73		~0	10.9				
	S.D.																	
S-3	0	0.0	17.5	82.5	9.46	1.65	235.6	1.25	6.24	86.19			~0	10.1				
1850m	10										4.04							
	20						168.2	1.33	4.46	81.68			~0	9.9				
	30																	
	40	0.0	15.4	84.6	9.50	1.50	183.9	1.31	4.87	82.97			~0	9.5				
	50										4.04							

Core	Depth		Texture (%)		Mean	Stand.	Water c.	Bulk d.	Void	Porosity	Shear str.	Specific	CaCO3	Org.	Att	erberg	L. (%)	Ac
No.	(cm)	Sand	Silt	Clay		Dev.	(%)	(g/cm3)	ratio	(%)	(kPa)	gravity	(%)	matt.(%)	PL	LL	PI	
S-3	60						185.5	1.30	4.92	83.10			~0	9.8				
	70																	
	80	0.0	30.0	70.0	9.09	1.83	190.1	1.30	5.04	83.44			1.7	10.4				
	90										2.22							
	100						214.8	1.27	5.69	85.06			~0	11.2				
	110										2.30							
	120						234.5	1.25	6.21	86.14			~0	14.4				
	130																	
	140	0.0	32.7	67.3	9.01	1.82	212.1	1.27	5.62	84.90	2.85		0.4	13.0				
	150																	
	160						201.9	1.29	5.35	84.25			~0	13.0				
	Ave.	0.0	23.9	76.1	9.27	1.70	203.0	1.29	5.38	84.19	3.09		~0	11.3				
	S.D.	0.0	8.7	8.7	0.25	0.16	23.3	0.03	0.62	1.53	0.90		~0	1.8				
	170																	
	180	2.8	36.0	61.2	8.63	2.17	135.3	1.39	3.59	78.19	3.09		5.1	9.5				
	190																	
	200						121.1	1.42	3.21	76.24			1.3	7.5				
	210																	
	220						153.6	1.35	4.07	80.28			2.9	9.9				
	230	0.0	41.7	58.3	8.65	1.85					3.49							
	240						163.7	1.33	4.34	81.27	3.33		3.9	9.2				
	250																	
	260	1.5	38.8	59.7	8.56	1.99	144.2	1.37	3.82	79.26			4.9	9.3				
	Ave.	0.5	27.2	63.2	8.05	1.63	173.2	1.32	4.59	82.11	2.94		3.6	7.8				
	S.D.	1.0	10.8	22.6	2.94	0.59	52.4	0.33	1.39	20.44	0.94		1.6	4.2				
S-4-1	0	0.2	32.0	67.8	8.99	1.86	278.9	1.22	7.39	88.08		2.62	2.6	11.2				
950m	10						245.1	1.25	6.50	86.66			2.5	11.2				
	20						222.0	1.27	5.88	85.47			2.6	10.8				

Core	Depth		Texture (%)		Mean	Stand.	Water c.	Bulk d.	Void	Porosity	Shear str.	Specific	CaCO3	Org.	Att	erberg	L. (%)	Ac
No.	(cm)	Sand	Silt	Clay		Dev.	(%)	(g/cm3)	ratio	(%)	(kPa)	gravity	(%)	matt.(%)	PL	LL	PI	
S-4-1	30						220.1	1.27	5.83	85.36	3.97		2.7	10.8				
	40	0.1	23.8	76.1	9.39	1.83	234.2	1.25	6.21	86.12		2.59	2.5	10.5				
	50						213.6	1.27	5.66	84.99			2.7	10.4				
	60						200.0	1.29	5.30	84.13			3.0	10.3				
	70						190.0	1.30	5.04	83.43			3.0	10.7				
	80	0.1	31.8	68.1	9.05	2.05	194.6	1.29	5.16	83.76		2.54	2.5	10.2				
	90						198.3	1.29	5.25	84.01			2.8	9.9				
	100						199.1	1.29	5.28	84.07	3.79		4.4	10.0				
	110						195.1	1.29	5.17	83.79	4.07		4.0	9.9				
	120	0.2	29.9	69.9	8.94	1.88	189.1	1.30	5.01	83.36		2.63	4.4	9.9				
	130						197.4	1.29	5.23	83.95	3.88		4.3	10.1				
	140						196.8	1.29	5.22	83.91	4.25		3.7	9.6				
	150						197.6	1.29	5.24	83.97	3.97		3.6	9.0				
	160	0.1	31.8	68.1	8.98	1.98	190.1	1.30	5.04	83.44		2.62						
	170						168.2	1.33	4.46	81.68	5.73		4.2	8.6				
	180	0.0	32.6	67.4	9.02	1.90	173.5	1.32	4.60	82.14			4.6	9.8				
	190											2.63						
	Ave.	0.1	30.3	69.6	9.06	1.92	205.5	1.28	5.44	84.33	4.24	2.61	3.3	10.2				
	S.D.	0.1	3.3	3.3	0.17	0.08	25.9	0.03	0.69	1.51	0.67	0.04	0.8	0.7				
S-4-2	0	0.2	24.7	75.1	9.29	1.82	233.4	1.25	6.19	86.08			2.5	11.5				
	10						207.7	1.28	5.50	84.62	2.18		3.4	10.6	56.0	133.6	77.6	1.03
	20						228.9	1.26	6.07	85.85	1.94		3.2	10.3				
	30						215.1	1.27	5.70	85.07	1.85		2.5	10.2				
	40	0.0	35.8	64.2	8.86	1.83	207.6	1.28	5.50	84.62	2.49		3.2	10.0	53.9	130.3	76.4	1.19
	50						224.1	1.26	5.94	85.59			3.2	9.7				
	60						208.9	1.28	5.54	84.70	2.22		3.1	9.9				
	70						195.9	1.29	5.19	83.85	2.86		4.0	9.9				

Core	Depth		Texture (%)		Mean	Stand.	Water c.	Bulk d.	Void	Porosity	Shear str.	Specific	CaCO3	Org.	Att	erberg	L. (%)	Ac
No.	(cm)	Sand	Silt	Clay		Dev.	(%)	(g/cm3)	ratio	(%)	(kPa)	gravity	(%)	matt.(%)	PL	LL	PI	
S-4-2	80	0.2	30.8	69.0	9.04	1.93	192.4	1.30	5.10	83.60	3.23		4.1	11.1	58.2	136.5	78.3	1.13
	90						182.9	1.31	4.85	82.90	3.88		3.2	10.0				
	100						184.5	1.31	4.89	83.02			2.9	10.1				
	110																	
	120														60.1	140.0	79.9	1.16
	130																	
	140																	
	150						167.9	1.33	4.45	81.65			4.3	10.8				
	160	0.0	19.7	80.3	9.43	1.76	153.1	1.35	4.06	80.23	5.82		3.5	10.4	61.4	140.0	78.6	0.98
	170						178.6	1.31	4.73	82.56	5.27		3.8	9.9				
	180						173.4	1.32	4.60	82.13	5.17		4.6	9.8	69.5	146.2	76.7	0.98
	190						182.7	1.31	4.84	82.88	4.80		3.5	9.8				
	200	0.0	21.8	78.2	9.53	1.96	171.2	1.32	4.54	81.94			4.8	9.5				
	210																	
	Ave.	0.1	26.6	73.4	9.23	1.86	194.6	1.30	5.16	83.60	3.48		3.5	10.2	59.9	137.8	77.9	1.08
	S.D.	0.1	6.6	6.7	0.28	0.08	23.2	0.03	0.61	1.64	1.45		0.7	0.5	5.0	5.1	1.2	0.09
S-5	0	0.0	16.3	83.7	9.75	1.79	218.8	1.27	5.80	85.29								
1400m	10										1.43							
	20	0.0	13.8	86.2	9.66	1.53	220.7	1.27	5.85	85.40	2.06							
	30										1.90							
	40	0.0	13.0	87.0	9.60	1.43	170.7	1.32	4.52	81.90	2.22							
	50										2.22							
	60						214.1	1.27	5.67	85.02	3.17							
	70										2.85							
	80	0.0	13.7	86.3	9.59	1.47	169.5	1.33	4.49	81.79	1.74							
	90										3.01							

Core	Depth		Texture (%)		Mean	Stand.	Water c.	Bulk d.	Void	Porosity	Shear str.	Specific	CaCO3	Org.	Att	erberg	L. (%)	Ac
No.	(cm)	Sand	Silt	Clay		Dev.	(%)	(g/cm3)	ratio	(%)	(kPa)	gravity	(%)	matt.(%)	PL	LL	PI	
S-5	100	0.0	10.4	89.6	10.0	1.64	170.4	1.32	4.52	81.87	5.47							
	110										4.04							
	120	0.0	16.5	83.5	9.51	1.55	177.8	1.31	4.71	82.49	3.96							
	130										4.68							
	140	0.0	16.2	83.8	9.70	1.69	193.0	1.30	5.11	83.65	3.65							
	150										2.46							
	160	0.0	15.0	85.0	9.55	1.50	180.8	1.31	4.79	82.73	5.39							
	170										5.55							
	180	0.0	14.6	85.4	9.55	1.53	180.1	1.31	4.77	82.68	4.76							
	190										5.39							
	200	0.0	18.0	82.0	9.42	1.58	189.6	1.30	5.02	83.40	5.71							
	210										5.07							
	220	0.0	13.5	86.5	9.72	1.54	191.3	1.30	5.07	83.52	4.60							
	230										4.76							
	240	0.0	24.4	75.6	9.27	1.75	187.8	1.30	4.98	83.27								
	Ave.	0.0	15.5	84.6	9.61	1.58	189.6	1.30	5.02	83.31	3.74							
	S.D.	0.0	3.5	3.5	0.18	0.11	18.0	0.02	0.48	1.26	1.42							
S-6-1	0	0.4	26.8	72.8	9.20	1.88	206.3	1.28	5.47	84.54		2.57	1.4	10.2				
1500m	10						186.8	1.30	4.95	83.19	2.40		2.0	9.7	54.7	136.6	81.9	1.13
	20						172.7	1.32	4.58	82.07	2.03		2.7	9.6				
	30						193.8	1.29	5.14	83.70	2.86		3.1	9.8				
	40	0.2	23.6	76.2	9.22	2.12	173.8	1.32	4.61	82.16		2.59	2.6	10.0				
	50						213.1	1.27	5.65	84.96	4.16		2.0	10.0	55.2	133.2	78.0	1.02
	60						193.2	1.30	5.12	83.66	3.79		2.3	9.6				
	70						192.2	1.30	5.09	83.59	4.25	2.58	2.7	10.1				
	80	0.3	24.4	75.3	9.34	2.28												

Core	Depth		Texture (%)		Mean	Stand.	Water c.	Bulk d.	Void	Porosity	Shear str.	Specific	CaCO3	Org.	Att	erberg	L. (%)	Ac
No.	(cm)	Sand	Silt	Clay		Dev.	(%)	(g/cm3)	ratio	(%)	(kPa)	gravity	(%)	matt.(%)	PL	LL	PI	
S-6-1	90														48.0	136.2	88.2	1.17
	100																	
	110																	
	120											2.56						
	130														50.0	130.8	80.8	1.12
	140																	
	150	1.2	26.6	72.2	9.16	2.01	205.8	1.28	5.45	84.51			1.1	11.8				
	160						207.3	1.28	5.49	84.60	3.51	2.55	~0	12.8				
	170						187.8	1.30	4.98	83.27	3.88		~0	14.3	49.5	133.2	83.7	1.39
	180	0.1	39.8	60.1	8.79	1.98	178.4	1.31	4.73	82.54			~0	13.7				
	Ave.	0.4	28.2	71.3	9.14	2.05	192.6	1.30	5.10	83.56	3.36	2.57	2.2	11.0	51.5	134.0	82.5	1.17
	S.D.	0.4	6.6	6.5	0.21	0.15	13.5	0.02	0.36	0.97	0.83	0.02	0.7	1.7	2.9	2.2	3.4	0.12
S-6-2	0	0.2	22.4	77.4	9.41	1.90	227.0	1.26	6.02	85.75			1.3	11.3				
	10						193.0	1.30	5.11	83.65	1.94		1.6	10.9	50.0	132.5	82.5	1.07
	20						204.9	1.28	5.43	84.45	2.59		2.2	10.3				
	30						183.9	1.31	4.87	82.97	4.90		2.0	9.8				
	40	0.1	21.4	78.5	9.47	1.88	178.8	1.31	4.74	82.57			2.0	9.7	50.9	136.3	85.4	1.09
	50						175.0	1.32	4.64	82.26	3.84		3.0	9.1				
	60						187.7	1.30	4.97	83.26	5.01		2.6	8.8				
	70						189.3	1.30	5.02	83.38	3.20		2.8	10.4				
	80	0.2	15.1	84.7	9.73	1.78	179.7	1.31	4.76	82.65	4.25		3.2	9.1	48.9	133.0	84.1	0.99
	90						176.7	1.32	4.68	82.40	5.45		2.6	8.8				
	100						185.4	1.30	4.91	83.09	3.84		2.4	8.6				
	110						199.0	1.29	5.27	84.06	6.84		2.2	8.1				
	120	0.2	31.0	68.8	9.05	1.98	212.1	1.27	5.62	84.90	8.32		2.7	8.4				
	130						169.8	1.33	4.50	81.82			2.4	8.3				

Core	Depth		Texture (%)		Mean	Stand.	Water c.	Bulk d.	Void	Porosity	Shear str.	Specific	CaCO3	Org.	Att	erberg	L. (%)	Ac
No.	(cm)	Sand	Silt	Clay		Dev.	(%)	(g/cm3)	ratio	(%)	(kPa)	gravity	(%)	matt.(%)	PL	LL	PI	
S-6-2																		
	Ave.	0.2	22.5	77.4	9.42	1.89	190.2	1.30	5.04	83.37	4.56		2.4	9.4	49.9	133.9	84.0	1.05
	S.D.	0.1	6.5	6.5	0.28	0.08	15.9	0.02	0.42	1.10	1.85		0.5	1.0				
S-7	0	0.0	29.7	70.3	9.00	1.70	179.6	1.31	4.76	82.64								
555m	10										3.49		3.0	11.6				
	20																	
	30										2.14							
	40	0.0	24.8	75.2	9.19	1.67	213.7	1.27	5.66	84.99			2.3	11.4				
	50																	
	60																	
	70										3.25							
	80	0.0	21.7	78.3	9.37	1.65	175.3	1.32	4.65	82.29			2.6	10.6				
	90																	
	100										3.57							
	110																	
	120	0.0	21.7	78.3	9.39	1.64	166.4	1.33	4.41	81.51	2.22		3.1	11.0				
	130																	
	140																	
	150																	
	160	0.0	22.8	77.2	9.29	1.57	169.8	1.33	4.50	81.82	3.57		3.4	10.5				
	170																	
	180																	
	190																	
	200	0.0	26.8	73.2	9.15	1.69	150.8	1.36	4.00	79.98	4.52		3.5	11.4				
	210																	
	220																	
	230																	

Core	Depth		Texture (%)		Mean	Stand.	Water c.	Bulk d.	Void	Porosity	Shear str.	Specific	CaCO3	Org.	Att	erberg	L. (%)	Ac
No.	(cm)	Sand	Silt	Clay		Dev.	(%)	(g/cm3)	ratio	(%)	(kPa)	gravity	(%)	matt.(%)	PL	LL	PI	
S-7	240	0.0	21.8	78.2	9.24	1.64	164.4	1.33	4.36	81.33	3.57		3.1	11.0				
	250																	
	260																	
	270	0.0	20.6	79.4	9.30	1.58	146.6	1.36	3.88	79.53			3.6	10.6				
	Ave.	0.0	23.7	76.3	9.24	1.64	170.8	1.33	4.53	81.76	3.29		3.1	11.0				
	S.D.	0.0	3.1	3.1	0.13	0.05	19.3	0.03	0.52	1.68	0.78		0.4	0.4				
S-8	0	0.0	15.5	84.5	9.55	1.54	193.6	1.29	5.13	83.69			1.3	10.7				
1355m	10										4.12							
	20						189.7	1.30	5.03	83.41			2.3	10.4				
	30																	
	40	0.9	21.2	77.9	9.31	1.71	183.4	1.31	4.86	82.94	3.73		0.9	10.2				
	50																	
	60						192.5	1.30	5.10	83.61			0.4	9.9				
	70																	
	80	0.0	14.0	86.0	9.60	1.50	191.4	1.30	5.07	83.53	1.90		1.3	9.8				
	90																	
	100						205.0	1.28	5.43	84.45	2.06		~0	10.2				
	Ave.	0.3	16.9	82.8	9.49	1.58	192.6	1.30	5.10	83.60	2.95		1.2	10.2				
	S.D.	0.5	3.8	4.3	0.16	0.11	7.1	0.01	0.19	0.49	1.14		0.7	0.4				
S-9	0	2.5	36.8	60.7	8.53	1.98	215.7	1.27	5.72	85.11			4.5	11.2				
650m	10																	
	20																	
	30										1.59							
	40	2.3	29.3	68.4	8.86	1.95	172.9	1.32	4.58	82.08			5.4	10.6				
	50																	

Core	Depth		Texture (%)		Mean	Stand.	Water c.	Bulk d.	Void	Porosity	Shear str.	Specific	CaCO3	Org.	Att	erberg	L. (%)	Ac
No.	(cm)	Sand	Silt	Clay		Dev.	(%)	(g/cm3)	ratio	(%)	(kPa)	gravity	(%)	matt.(%)	PL	LL	PI	
S-9	60																	
	70										3.09							
	80	2.7	29.4	67.9	8.89	2.12	177.6	1.31	4.71	82.48			5.9	11.3				
	90																	
	100																	
	110										4.04							
	120	2.7	25.0	72.3	9.01	1.97	163.8	1.33	4.34	81.28			6.4	10.9				
	130										6.98							
	140																	
	150																	
	160	3.0	32.0	65.0	8.64	1.93	183.6	1.31	4.87	82.95			3.4	10.2				
	170																	
	180																	
	190																	
	200	2.8	32.6	64.6	8.72	1.98	167.3	1.33	4.43	81.60			4.2	10.9				
	210																	
	220																	
	230																	
	240	2.2	34.2	63.6	8.65	2.01	169.5	1.33	4.49	81.79			4.6	10.7				
	250																	
	260																	
	270	3.1	43.6	53.3	8.27	2.00	158.5	1.34	4.20	80.77			5.1	10.4				
	Ave.	2.7	32.9	64.5	8.70	1.99	176.1	1.32	4.67	82.26			4.9	10.8				
	S.D.	0.3	3.8	5.7	0.23	0.06	17.8	0.02	0.47	1.34			1.0	0.4				
S-10	0	95.2	4.8	0.0	2.25	0.77	38.8	1.84	1.03	50.70								
220m	10																	

Core	Depth		Texture (%)		Mean	Stand.	Water c.	Bulk d.	Void	Porosity	Shear str.	Specific	CaCO3	Org.	Att	erberg	L. (%)	Ac
No.	(cm)	Sand	Silt	Clay		Dev.	(%)	(g/cm3)	ratio	(%)	(kPa)	gravity	(%)	matt.(%)	PL	LL	PI	
S-10	20	97.9	2.1	0.0	1.92	0.66	28.6	1.96	0.76	43.11								
	30																	
	40	98.1	1.9	0.0	1.79	0.63	29.0	1.95	0.77	43.45								
	50																	
	60	98.1	1.9	0.0	1.75	0.64	28.4	1.96	0.75	42.94								
	70																	
	80	97.5	2.5	0.0	1.73	0.72	28.2	1.96	0.75	42.77								
	90																	
	100	97.0	3.0	0.0	1.73	0.81	26.4	1.99	0.70	41.16								
	110						25.7	2.00	0.68	40.51								
	120	96.7	3.3	0.0	1.70	0.89												
	Ave.	97.2	2.8	0.0	1.84	0.73	29.3	1.95	0.78	43.52								
	S.D.	1.0	1.0	0.0	0.20	0.10	4.4	0.05	0.12	3.35								
S-11-1	0	96.6	1.3	1.7	2.76	1.20	24.0	2.03	0.64	38.88		2.68	1.8	4.9				
260m	10						30.0	1.94	0.80	44.29			2.1	2.2				
	20						32.3	1.91	0.86	46.12			3.0	1.8				
	30						30.2	1.94	0.80	44.45			2.4	1.7				
	40	91.7	3.0	5.0	3.12	1.86	34.4	1.88	0.91	47.69		2.65	2.9	1.9				
	50						36.4	1.86	0.96	49.10			2.5	1.9				
	60						34.7	1.88	0.92	47.90			2.6	1.9				
	70						33.6	1.89	0.89	47.10			2.7	2.0				
	80	96.7	3.0	0.0	2.68	0.47	36.6	1.86	0.97	49.24		2.66	2.0	1.7				
	90						33.2	1.90	0.88	46.80			2.7	2.4				
	100						35.1	1.88	0.93	48.19			3.5	2.8				
	110						33.9	1.89	0.90	47.32			2.9	2.7				
	120	92.6	2.9	4.1	3.06	1.74	32.8	1.90	0.87	46.50		2.69	3.3	2.6				

Core	Depth		Texture (%)		Mean	Stand.	Water c.	Bulk d.	Void	Porosity	Shear str.	Specific	CaCO3	Org.	Att	erberg	L. (%)	Ac
No.	(cm)	Sand	Silt	Clay		Dev.	(%)	(g/cm3)	ratio	(%)	(kPa)	gravity	(%)	matt.(%)	PL	LL	PI	
S-11-1	130						30.9	1.93	0.82	45.02			3.1	2.9				
	140	92.4	3.7	4.3	3.05	1.70	30.9	1.93	0.82	45.02			3.1	2.8				
	Ave.	94.0	2.8	3.0	2.93	1.39	32.6	1.91	0.86	46.24		2.67	2.7	2.4				
	S.D.	2.4	0.9	2.1	0.20	0.57	3.2	0.04	0.08	2.57		0.02	0.5	0.8				
S-11-2	0	97.6	2.0	0.0	2.81	0.52	31.2	1.92	0.83	45.26			14.7	2.2				
	10						29.2	1.95	0.77	43.62			5.8	1.5				
	20	93.4	3.7	3.1	3.07	1.48	30.4	1.93	0.81	44.62			12.2	1.4				
	Ave.	95.5	2.9	1.6	2.94	1.00	30.3	1.94	0.80	44.50			10.9	1.7				
S-12-1	0	0.5	34.5	65.0	8.91	2.02	195.6	1.29	5.18	83.83		2.52	2.9	10.4				
770m	10						198.6	1.29	5.26	84.03	1.58		2.7	10.4	51.4	122.5	71.1	1.09
	20						190.2	1.30	5.04	83.44	1.85		2.7	10.4				
	30						299.2	1.21	7.93	88.80	2.03		3.5	10.5				
	40	0.0	29.3	70.7	9.09	2.07	177.9	1.31	4.71	82.50		2.57	3.8	10.5				
	50						172.6	1.32	4.57	82.06	3.70		3.8	10.4	57.4	130.3	72.9	1.03
	60						173.6	1.32	4.60	82.14	3.23		4.3	10.7				
	70						212.6	1.27	5.63	84.93	4.44		5.4	10.7				
	80	0.0	35.4	64.6	8.93	2.33	162.4	1.34	4.30	81.14		2.59	5.3	10.6	57.3	123.7	66.4	1.03
	90						181.6	1.31	4.81	82.80	4.07		4.8	10.1				
	100						183.7	1.31	4.87	82.96	4.07		6.1	10.4				
	110																	
	120																	
	130																	
	140																	
	150						159.9	1.34	4.24	80.91			6.2	11.0				

Core	Depth		Texture (%)		Mean	Stand.	Water c.	Bulk d.	Void	Porosity	Shear str.	Specific	CaCO3	Org.	Att	erberg	L. (%)	Ac
No.	(cm)	Sand	Silt	Clay		Dev.	(%)	(g/cm3)	ratio	(%)	(kPa)	gravity	(%)	matt.(%)	PL	LL	PI	
S-12-1	160	0.5	32.8	66.7	9.05	2.01	162.4	1.34	4.30	81.14		2.57	6.4	10.4				
	170						159.3	1.34	4.22	80.85	7.21		6.5	10.3	55.9	124.2	68.3	1.02
	180						152.5	1.35	4.04	80.16	7.95		5.2	10.0				
	190						170.7	1.32	4.52	81.90	7.85		5.1	10.0				
	200	0.5	19.7	79.8	9.45	1.80	164.0	1.33	4.35	81.29		2.56	4.1	10.5				
	210						150.0	1.36	3.98	79.90			4.8	9.9	64.1	133.9	69.8	0.87
	220						157.3	1.34	4.17	80.65	5.08		4.4	9.6				
	230						174.3	1.32	4.62	82.20	5.36		4.4	10.0				
	240	0.7	35.8	63.5	8.87	2.10	162.6	1.34	4.31	81.16		2.56	4.5	9.9				
	250						171.5	1.32	4.54	81.96	5.64		3.9	9.4	62.2	130.0	67.8	1.07
	260						166.8	1.33	4.42	81.55	5.64		3.9	9.6				
	270						159.1	1.34	4.22	80.83			4.3	9.6	60.0	127.7	67.7	1.04
	280	0.3	34.9	64.8	9.06	2.22	154.6	1.35	4.10	80.38		2.54	4.5	9.8				
	Ave.	0.4	31.8	67.9	9.05	2.08	176.5	1.32	4.68	82.14	4.65	2.56	4.5	10.2	58.3	127.5	69.2	1.02
	S.D.	0.3	5.8	5.8	0.19	0.17	29.9	0.03	0.79	1.88	2.04	0.02	1.1	0.4	4.2	4.2	2.3	0.07
S-12-2	0	0.5	34.2	65.3	8.92	2.01	256.1	1.24	6.79	87.16			2.3	12.4				
	10						240.4	1.25	6.37	86.43			1.6	10.6				
	20						208.5	1.28	5.53	84.67			2.4	9.6				
	30	0.6	34.1	65.3	8.98	2.03	219.9	1.27	5.83	85.35			2.8	9.5				
	40						216.1	1.27	5.73	85.13			2.6	9.3				
	50						225.5	1.26	5.98	85.66			3.3	9.0				
	60	0.4	33.7	65.9	8.99	2.06	195.0	1.29	5.17	83.79			4.4	9.0				
	70																	
	Ave.	0.5	34.0	65.5	8.96	2.03	223.1	1.27	5.91	85.46			2.8	9.9				
	S.D.	0.1	0.3	0.3	0.04	0.03	20.2	0.02	0.54	1.11			0.9	1.2				

Core	Depth		Texture (%)		Mean	Stand.	Water c.	Bulk d.	Void	Porosity	Shear str.	Specific	CaCO3	Org.	Att	erberg	L. (%)	Ac
No.	(cm)	Sand	Silt	Clay		Dev.	(%)	(g/cm3)	ratio	(%)	(kPa)	gravity	(%)	matt.(%)	PL	LL	PI	
S-13-1	0	89.2	5.3	5.7	3.40	1.89	38.6	1.84	1.02	50.57			4.7	2.9				
230m	10						49.5	1.74	1.31	56.74			5.3	4.2				
	20	30.5	50.0	19.0	5.98	2.58	58.6	1.67	1.55	60.83			5.9	2.9				
S-13-2	0	29.0	46.4	24.6	6.29	2.72	37.4	1.85	0.99	49.78		2.67	7.9	4.0				
	10						67.0	1.62	1.78	63.97	8.13		13.0	6.7	30.8	70.0	39.2	1.59
	20						75.4	1.57	2.00	66.65	7.82		13.0	7.0				
	30						76.7	1.57	2.03	67.02			11.4	7.5				
	40	22.7	48.3	28.6	6.80	2.85	74.8	1.58	1.98	66.47		2.66	11.2	7.8				
	50						80.7	1.55	2.14	68.14	11.36		10.4	7.7	33.5	73.6	40.1	1.40
	60						72.2	1.59	1.91	65.67	11.69		12.0	7.5				
	70						77.0	1.57	2.04	67.11	11.69		11.8	8.1				
	80	16.3	51.5	32.5	7.06	2.70	77.6	1.56	2.06	67.28		2.66	11.3	8.0				
	90						72.4	1.59	1.92	65.74	12.02		11.8	7.6	34.5	67.1	32.6	1.00
	100						71.7	1.59	1.90	65.52	13.03		15.2	6.7				
	110						75.1	1.58	1.99	66.56	10.69		10.9	7.1				
	120	21.1	50.4	28.6	6.70	2.76						2.67	10.2	7.4				
	130												11.2	7.1	33.2	60.1	26.9	0.94
	140												10.9	7.8				
	150												10.7	6.9				
	160	15.8	40.8	43.2	7.75	2.87						2.68	10.7	6.8				
	170												10.0	6.8	38.3	63.1	24.8	0.57
	180												10.7	7.7				
	190												10.7	7.2				
	200	13.6	44.4	41.6	7.66	2.74						2.66	10.6	7.4				
	210												11.0	7.8	30.0	57.6	27.6	0.66

Core	Depth		Texture (%)		Mean	Stand.	Water c.	Bulk d.	Void	Porosity	Shear str.	Specific	CaCO3	Org.	Att	erberg	L. (%)	Ac
No.	(cm)	Sand	Silt	Clay		Dev.	(%)	(g/cm3)	ratio	(%)	(kPa)	gravity	(%)	matt.(%)	PL	LL	PI	
S-13-2	220												10.8	8.0				
	230	14.8	44.5	40.5	7.51	2.73							10.4	7.5				
	240																	
	Ave.	19.0	46.6	34.2	7.11	2.77	71.5	1.89	1.89	64.99	10.80	2.67	11.2	7.3	33.4	65.2	31.8	1.03
	S.D.	5.5	3.7	7.5	0.55	0.07	11.3	0.08	0.30	4.91	1.87	0.01	1.3	0.8	2.7	5.6	6.0	0.40
S-14	0	5.7	48.5	45.8	7.98	2.60	28.2	1.96	0.75	42.77		2.67	11.8	4.7				
130m																		
	10	95.5	3.0	1.0	2.85	1.05	13.1	2.24	0.35	25.77			2.8	1.4				
	20						19.8	2.10	0.52	34.41			2.0	1.4				
	30						27.5	1.97	0.73	42.15			3.7	2.3				
	40	89.6	5.5	4.5	3.30	1.74	36.3	1.86	0.96	49.03		2.70	7.8	3.3				
	50						30.2	1.94	0.80	44.45			5.1	2.4				
	60						32.3	1.91	0.86	46.12			5.3	2.7				
	70						30.2	1.94	0.80	44.45			4.0	2.2				
	80	92.9	5.0	2.0	2.95	1.33	29.7	1.94	0.79	44.04		2.70	3.6	2.0				
	90						28.4	1.96	0.75	42.94			3.6	2.4				
	100	93.6	4.0	2.0	3.00	1.32	27.0	1.98	0.72	41.71			1.6	1.6				
	110																	
	Ave.	92.9	4.4	2.4	3.03	1.36	27.5	1.98	0.73	41.51			4.0	2.2				
	S.D.	2.5	1.1	1.5	0.19	0.28	6.6	0.11	0.17	6.68			1.8	0.6				
S-15-1	0	97.9	2.0	0.0	2.66	0.43	31.2	1.92	0.83	45.26			9.6	2.8				
140m	10						28.1	1.97	0.74	42.68			8.5	2.3				
	20						26.5	1.99	0.70	41.25			8.6	2.0				
	30						26.6	1.99	0.70	41.35			5.4	2.3				
	40	93.9	2.5	3.5	2.90	1.60	29.5	1.95	0.78	43.88			10.8	2.1				
	Ave.	95.9	2.3	1.8	2.78	1.02	28.4	1.96	0.75	42.88			8.6	2.3				
	S.D.	2.8	0.4	2.5	0.17	0.83	2.0	0.03	0.05	1.71			2.0	0.3				

Core	Depth		Texture (%)		Mean	Stand.	Water c.	Bulk d.	Void	Porosity	Shear str.	Specific	CaCO3	Org.	Att	erberg	L. (%)	Ac
No.	(cm)	Sand	Silt	Clay		Dev.	(%)	(g/cm3)	ratio	(%)	(kPa)	gravity	(%)	matt.(%)	PL	LL	PI	
S-15-2	0	97.4	2.6	0.4	2.68	0.46	34.3	1.89	0.91	47.62		2.68	19.6	1.9				
	10						30.9	1.93	0.82	45.02			16.8	2.1				
	20						28.7	1.96	0.76	43.20			15.1	1.9				
	30	98.7	1.0	0.0	2.53	0.36	29.1	1.95	0.77	43.54			15.3	1.8				
	40						27.9	1.97	0.74	42.51		2.69	14.5	1.5				
	50						27.3	1.98	0.72	41.98			14.1	1.8				
	60	96.5	3.0	0.0	2.57	0.48	27.2	1.98	0.72	41.89			17.4	1.8				
	Ave.	97.5	2.2	0.1	2.59	0.43	29.3	1.95	0.78	43.68			16.1	1.8				
	S.D.	1.1	1.1	0.2	0.08	0.06	2.5	0.03	0.07	2.04			1.9	0.2				